Physics – Uspekhi **45** (11) 1109 – 1129 (2002)

REVIEWS OF TOPICAL PROBLEMS PACS number: 41.75.Ak

Collective ion acceleration in systems with a virtual cathode

A E Dubinov, I Yu Kornilova, V D Selemir

DOI: 10.1070/PU2002v045n11ABEH001255

Contents

Abstract. The current status of research and development in the realm of physics and technology of collective ion acceleration in systems with a virtual cathode (VC) is reviewed. Three major acceleration methods and devices developed on their basis are considered: reflex triodes and their modifications, gas-filled vircators, and vacuum vircators with a Luce diode. Experimental data are outlined and the principal physical models interpreting these data are described. New ion acceleration techniques whose realization involves the production and disappearance of the VC are also discussed. All methods of collective ion acceleration are compared and the possible ways for the further development of this promising scientific field are highlighted.

1. Introduction

The objective of our review is to consider and analyze the physics and technology of collective ion acceleration in systems involving high-current electron beams with a virtual cathode (VC).

The work on developing the techniques of collective ion acceleration began more than 40 years ago. A characteristic feature of these techniques is that the main part is played by the interaction of accelerated particles with self-consistent collective space-charge fields or currents caused by the aggregate of plasma electrons, relativistic beams, rings, bunches, and other formations. The prevalence of collective processes in accelerating systems based on similar techniques substantially rises the peak intensities of the accelerating fields (up to $\sim 10^6$ V cm^{-1}) and the limiting currents of particles being accelerated (up to ~ 1 MA), which makes it possible to generate high-current ion beams with a power up to ~ 1 TW. The prospects for using these beams is generally recognized and the field of application is very broad — controlled nuclear fusion [1, 2], development of high-power pulsed neutron sources [3], pumping of high-power lasers [4], etc.

At present, of greatest interest are the collective techniques harnessing the VC phenomenon. First, these techniques are still in the stage of the quest for solutions unlike, for instance, the completely elaborated ion acceleration technique employing relativistic electron rings [5], and therefore these techniques are permanently enriched with new theoretical and experimental findings. Second, these techniques are in the lead as regards the limiting ion currents attained (up to 1 MA in reflex diodes) and the energy of accelerated beams (up to 45 MeV per nucleon in Luce diodes), which arouses active interest in them.

Three principal schemes of collective ion acceleration are recognized in VC systems, which have mostly been studied and have found the widest application in experiments: diode type reflecting systems (RSs), gas-filled vircators, and vacuum vircators with ion production at the anode (Luce diodes or vircators with a plasma anode). A start on the development of these techniques was made in the early 1970s. Suffice it to recall in this connection the transactions of the *Ist* and *IInd Symposia on Collective Ion Acceleration Techniques*

A E Dubinov, I Yu Kornilova, V D Selemir Russian Federal Nuclear Center — All-Russia Scientific Research Institute of Experimental Physics (VNIIÉF), prosp. Mira 37, 607188 Sarov, Nizhniĭ Novgorod Region, Russian Federation
Tel. (7-83130) 4 51 44. Fax (7-83130) 4 53 84
E-mail: dubinov@ntc.vniief.ru

Received 28 February 2002, revised 27 June 2002
Uspekhi Fizicheskikh Nauk **172** (11) 1225 – 1246 (2002)
Translated by E N Ragozin; edited by A Radzig

(Dubna, 1972 and 1976), the *Workshops on the Problems of Collective Acceleration Technique* (Dubna, 1982), the *VIth* and *VIIth All-Union Workshops on Charged Particle Accelerators* (Dubna, 1979 and 1983), which saw the publication of many basic papers in the field of collective ion acceleration using electron beams with a VC.

Let us see what underlies the collective acceleration techniques. According to the Child – Langmuir law, the electron and ion current densities in a diode are defined by the expression

$$j_{\mathrm{e,i}}^{\mathrm{ChL}} = \frac{\sqrt{2}\,\alpha}{9\pi}\left(\frac{eZ_{\mathrm{e,i}}}{m_{\mathrm{e,i}}}\right)^{1/2}\frac{U_0^{3/2}}{d^2}\,, \qquad (1)$$

where $Z_{\mathrm{e,i}}$ and $m_{\mathrm{e,i}}$ are the charge and rest mass of electrons and ions, U_0 is the voltage applied to the diode gap, d is the gap width, and the value of α is determined by the character of steady electron – ion streams ($\alpha = 1.86$ in the bipolar mode). From expression (1) it follows that the current in a bipolar diode is carried primarily by electrons (up to 95 – 99%) rather than heavy positive ions. This brings up the problem of suppressing the electron current in the accelerating gap. One way to solve this problem was proposed and realized by Humphries et al. [6] in 1974. The suppression of the electron current component is attained in a diode by way of multiple electron oscillations between the cathode and the VC. This phenomenon underlies all existing RSs. We also note some other ways of suppressing the electron current in a diode: magnetic insulation of electrons in magnetized diodes [7, 8], and increasing the cathode-to-anode electron transportation distance in diodes with electron beam pinching [9].

Techniques for producing the high-power ion beams (HPIBs) in gas-filled vircators and vacuum vircators with ion production at the anode are based on the acceleration of a high-current electron beam whose space-charge field also entrains positive ions in the accelerating motion. These techniques of collective acceleration take advantage of the fact that the electron mass is far less than the mass of an ion to be accelerated, and therefore the initial electron acceleration is easier to accomplish. We note that the external electric field and hence the acceleration rate cannot be infinitely raised in the case of conventional acceleration because of the risk of the breakdown in the accelerating gap, whereas in the case of collective acceleration this problem can be partly or completely removed.

Our review is dedicated to the description of the above techniques of collective ion acceleration. In Section 2 we consider the way of collective ion acceleration in diode RSs. The types of existing diode RSs and their operating principles are analyzed. A comparison analysis of different ion sources is given. The fields of application of the RSs are specified. In Section 3 we discuss the technique of collective ion acceleration in gas-filled vircators. We give the main theoretical models and calculated results and compare them with the experimental data. The methods for synchronizing the motion of the VC front with the motion of ions being accelerated are also described. In Section 4 we consider the method of collective ion acceleration in vacuum vircators with ion production at the anode. Conventional Luce diodes and their modifications are described. The papers in which a self-consistent theory of this acceleration technique was constructed are also presented. Section 5 acquaints the reader with some other little-known techniques of collective ion acceleration in electron beams with a VC, and the most promising ones are laid out. In Section 6, we give the summary comparison of the techniques considered and point to the possible ways for the further development of the physics and technology of collective ion acceleration in VC-based systems.

2. Collective ion acceleration in diode type reflecting systems

2.1 Diode RSs and their classification

The idea of producing HPIBs in diode RSs was first proposed and realized by Humphries et al. [6] in 1974. A proton beam with parameters $E_{\mathrm{i}} = 100$ keV, $I_{\mathrm{i}} = 500$ A, and $\tau = 50$ ns was obtained in the geometry of a reflex triode (RT) (Fig. 1b). In the same year, Huff and Smith [10] published the results of experiments on HPIB generation in a twin diode (TD) (Fig. 1a). The new avenue of investigation into accelerating technology then made great strides and, before long, other types of diode systems put in their appearance, which were based on the principle of reflection: asymmetric triodes, reflex tetrodes (Figs 1c – e).

The operating principle of these systems is as follows. Upon application of a high-voltage pulse to the anode, electrons are emitted by one (in systems with a VC) or two (in systems with a TD) cathodes. Subsequently they are accelerated in the electric field of the A – C gap and start to oscillate in the potential well and intersect the anode (10 – 100-μm thick) which is rather transparent for them. The anode is usually made from a material with a high content of hydrogen and constitutes a good plasma source. The energy deposited by electrons when intersecting the anode goes into heating the anode material and producing the near-surface plasma. The ions extracted from the anode plasma are accelerated in the electric fields of the A – C and A – VC gaps and brought out through semitransparent cathodes from the diode space. The system is usually embedded in a longitudinal magnetic field (several kilogauss) to eliminate the electron losses at the walls and the anode holder.

As regards the number of beams generated, RSs are classified as symmetric (two ion beams) and asymmetric (one ion beam). Among the symmetric RSs are the TD and RT ones (Figs 1a and 1b) which were intensively studied

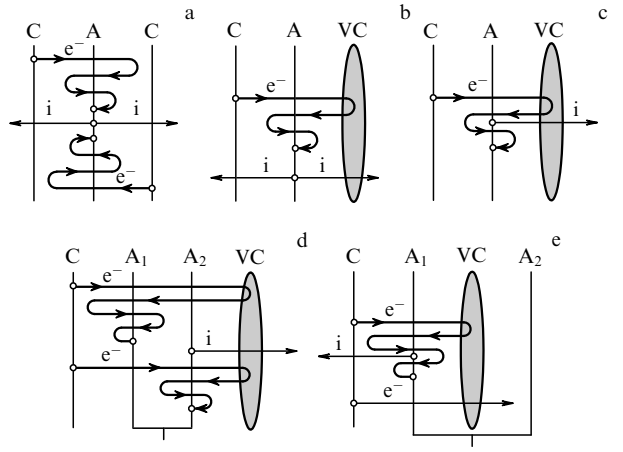

Figure 1. Schematics of the RS: (a) twin diode (TD); (b) symmetric RT; (c) asymmetric RT, and (d, e) tetrodes.

during the first 5–7 years of pursuance of the line of investigation under review. The results obtained were published in well-written reviews [11, 12]. Among the drawbacks to these systems are (i) the low-impedance mode of operation, whereby the mismatch to the forming supply line of the accelerator is responsible for the production of an ion beam with an incomplete energy content, and (ii) limitation of acceleration efficiency by a value of $\leqslant 50\%$ because of the second ion beam (usually wasted) moving towards the real cathode. Largely devoid of the above drawbacks are asymmetric RSs: an asymmetric TR wherein one side of the anode is a good ion source, and modifications of a tetrode (Figs 1c–e).

2.2 Comparison analysis of symmetric and asymmetric RSs

We briefly consider the processes accompanying HPIB production in symmetric and asymmetric RSs. Theoretical investigations into the operation of symmetric RSs [13–16] revealed that the behavior of ion j_i and electron j_e diode current densities under some conditions is characterized by divergence and the zero value of the triode impedance. With these conditions may be grouped some specific values of the contribution Δ from electron fluxes scattered in the anode [15], of the average number of anode intersections η by the oscillating electrons prior to their absorption in the anode [13], etc. Figure 2 serves to exemplify the divergence.

The cause of divergence lies with a drastic decrease of the triode impedance due to the charge neutralization of the A–C gap. This phenomenon is clearly illustrated in Fig. 3.

The dependence of the ion current on the triode voltage is different from the relationship $I_i \sim U^{3/2}$ and, with the inclusion of electron scattering in the anode foil, is described by the relationship $I_i \sim U^{3.5}$ [15].

The experimental studies [6, 17–25] of symmetric RSs confirmed the occurrence of processes predicted by stationary models. However, the experimental parameters of these systems were observed to quantitatively differ from the calculated ones. A research on the operation of real RSs revealed that this discordance is due to several factors. First, the processes in real symmetric RSs are immanently transient, whereas theoretical models cover stationary processes. Depending on specific experimental conditions, the nonstationarity may manifest itself in the periodic ion-beam generation [22], in collective acceleration of a portion of the ions to energies which are many times the parameter eZ_iU_0 [26], in the oscillations of the spatial charge density, and in microwave generation [27]. Second, the voltage across the A–C gap changes in real facilities, while in theoretical models it is assumed constant. In experiments, when the triode impedance drops it mismatches to the forming element of the accelerator, with the effect that the voltage across the anode decreases. This in turn leads to a reduction in η, which has a significant effect on the output parameters of the ion beam. The electron beam losses at the walls also make a contribution to the quantitative disagreement.

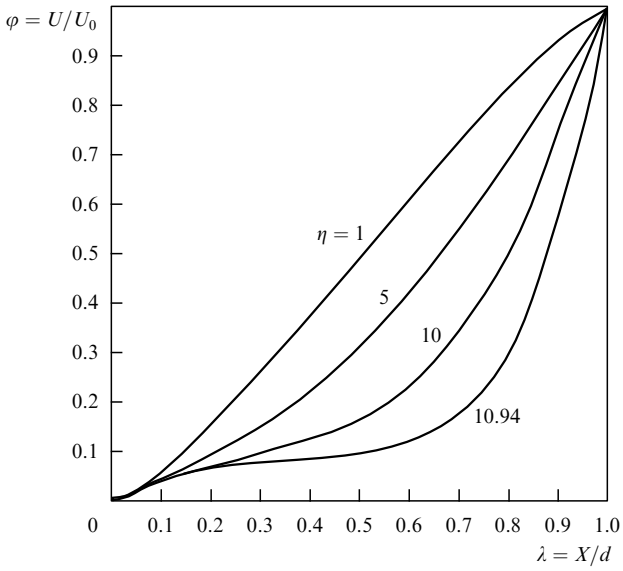

Figure 3. Coordinate dependence of the potential for the electron flux distribution function corresponding to curve *2* in Fig. 2 [13].

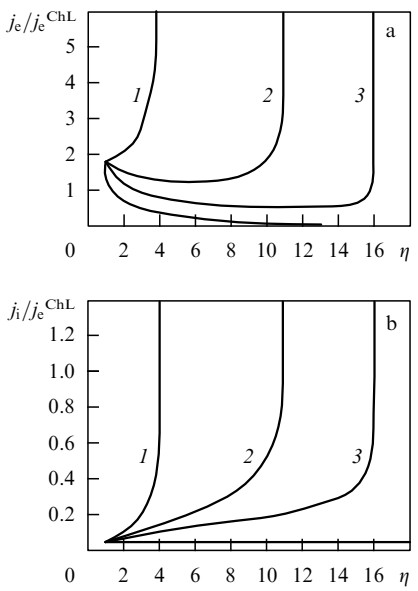

Figure 2. Dependences of j_e/j_e^{ChL} and j_i/j_e^{ChL} on the average number of anode intersections η for different electron flux distribution functions in a symmetric triode [13].

Asymmetric RSs are characterized by different dynamics of accumulation and propagation of the spatial charge. In an asymmetric RT, where only one anode surface (usually on the VC side) is a good ion source, the ion beam travels only towards the VC. Therefore, two regions can be distinguished in an asymmetric triode: (i) the region of purely electron streams (the A–C gap), and (ii) that of electron–ion streams (the A–VC gap).

Tetrodes represent a modification of asymmetric RTs. They also generate a single ion beam. The tetrode scheme was first proposed in 1978 [28, 29]. The basic idea of this scheme involves the use of two anodes (A_1 and A_2), one of which (A_2) is a good ion source and is usually arranged on the VC side. In this geometry, the electric field of the cathode does not penetrate to the ion-emitting surface of the A_2 anode, with the result that the HPIB is produced only in the direction of the VC. Under this tetrode geometry, in the stationary state there exist three groups of oscillating electrons: two groups vibrate about one of the anodes, and one group vibrates about two anodes. As the energy is lost, electrons transfer from the latter group to the former two.

A somewhat different tetrode scheme (Fig. 1e) was considered in Ref. [30]. Its distinctive feature is that the VC is formed between the anodes. In this case there are two groups of oscillating electrons, one of which vibrates about the A_1 anode, and the other about the A_2 anode. With this geometry, the ion beam travels towards the real cathode.

The theoretical investigation of the proposed stationary asymmetric models reduces to the simultaneous solution of the Poisson equations written down for the selected regions of the diode system. Arbuzov et al. [31] considered a one-dimensional model of the steady-state mode for an asymmetric RT in the nonrelativistic approximation. Figure 4 gives the results of numerical simulations for different electron distribution functions. With reference to the figure, with an increase in the number of anode intersections η and irrespective of the electron flux distribution function, the ion current rises with a simultaneous lowering of the electron current, and in the limit $\eta \to \infty$ their values coincide. Therefore, the divergence of ion and electron currents and, accordingly, the impedance collapse are not observed in an asymmetric RT. Similar results were also obtained for two tetrode schemes [30, 32]. Hence it follows that asymmetric RSs allow an operation in the high-impedance mode. This mode of operation can be employed for laser pumping, neutron pulse production, etc.

As regards the magnitude of generated currents for the common parameters, symmetric RSs are an indisputable advantage. One can see from Fig. 2 that the ion currents in symmetric RSs can far exceed the ChL limit (by a factor of 6 – 60, according to experimental data), whereas in asymmetric RSs their values are always below the ChL limit (see Fig. 4). The latter is attributable to the large spatial charge of purely electron regions in asymmetric RSs. Reflecting systems with a single ion beam rank highest in efficiency, but the efficiencies attainable in reality so far remain below the calculated ones: 45% for symmetric RSs, and 70% for the asymmetric ones [12].

The highest ion beam currents attained in diode RSs to date amount to $\leqslant 1$ MA at a power level of $\leqslant 1$ TW. Experimental investigations revealed a strong dependence of the ion yield on the parameters of a diode system, like the anode material and structure [6, 17, 21, 25], the operating voltage [20, 22], and the amplitude of an external magnetic field [18]. The geometric tetrode parameters (the total thickness of the anodes, the electrode-to-electrode distance ratio) optimized for a maximum ion yield were theoretically evaluated in Refs [30, 32].

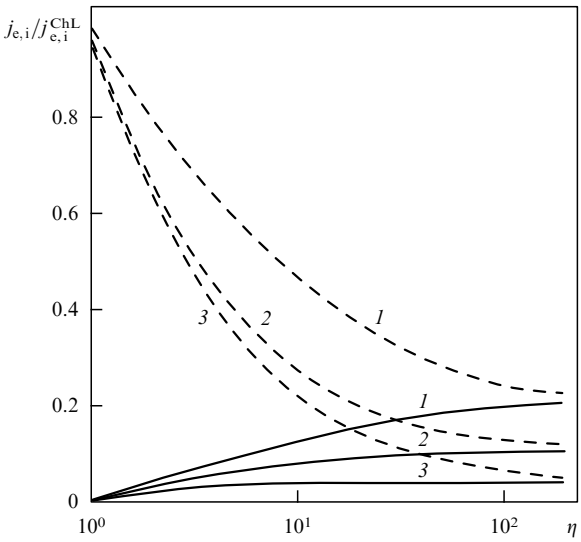

Figure 4. Dependences of j_e/j_e^{ChL} (– – –) and j_i/j_e^{ChL} (——) on the average number of anode intersections η for different electron flux distribution functions in an asymmetric triode [31].

2.3 Techniques of anode-plasma production, and composition of ion beams

In the design of a reflecting system, the problem of developing a reliable and simple anode-plasma source is not least in importance. Three main ways of anode-plasma production can be distinguished: (i) by electron bombardment of thin conducting anodes or anodes covered with dielectric films; (ii) due to surface breakdown of a massive metallodielectric anode, and (iii) using an external source at the anode.

The first two ways have significant drawbacks. The operation with thin conducting anodes is characterized by a substantial delay of the onset of ion beam generation after the application of a voltage pulse. Investigations into high-current ion beam (HCIB) generation in a triode for different anode materials [25] revealed that this delay for 10 – 110-μm thick aluminum foils comprises about 30 ns. The delay corresponds to the time it takes to attain a certain value of specific energy addition to the anode, effected by the oscillating electrons. According to the totality of experimental data, this value amounts to 1 – 3 kJ g^{-1}.

When operating with the anodes made up of a metal skeleton covered with a dielectric film 15 – 110 μm in thickness, the delay time was significantly shorter (5 – 10 ns). The authors attributed the early anode-plasma production to the surface dielectric-film breakdown at the leading edge of the voltage pulse. However, the disadvantage of film anodes, like the foil ones though, is their short durability limited, at best, to several operating pulses.

Recourse to a massive (much thicker than the electron mean free path) metallodielectric anode permits the RS to be operated in a multipulse mode. In these RSs, electrons vibrate through the openings in the anode. The source of ions is the plasma produced in the surface breakdown of the anode dielectric. Bystritskiĭ et al. [25] observed that in this case the behavior of voltage and total current in the triode is the same as in the case of an anode with a dielectric film, but the operating efficiency is somewhat lower ($\leqslant 30\%$ as compared with $\leqslant 45\%$).

The technique of anode-plasma production with the accelerator charging prepulse was proposed to reduce the time delay of the anode plasma production relative to the start of a high-voltage pulse. In the experiments of this kind [33, 34], use was made of a compound anode whose elements were made of brass in the form of similar cylinders connected together by dielectric pins. One half of the anode was connected to the anode holder, and the other to the charging inductor of the double forming line (DFL). To control the steepness of the leading edge and duration of the prepulse, a switching tube was employed in the DFL circuit. In this scheme, the breakdown of the gap ($\sim$ 1 mm) of the compound anode and the plasma production occur prior to the delivery of a high-voltage pulse to the anode. The preliminary plasma production should seemingly bring about a strong reduction of the time delay. However, this was not confirmed by experiments. The plasma produced with the prepulse is not dense enough for HPIB generation. This is explained by the

plasma deceleration in its motion normally to the magnetic field to the paraxial anode region and also by the short duration of this motion (~ 400 ns) until the arrival of the main pulse. For an average velocity of plasma motion at a level of $\leqslant 10^6$ cm s^{-1}, the estimated distance traversed amounts to several tenths of a centimeter. Bystritskiĭ et al. [34] observed that the delay time of HPIB production relative to the start of the voltage pulse was equal to 30 – 40 ns. Hence, the authors concluded that the main anode-plasma production took place during the running voltage pulse through direct heating of the anode material by the oscillating electrons.

The greatest promise is exhibited by the method of plasma production due to the breakdown of the dielectric insert or vacuum gap of the compound anode by an external source. As shown in Ref. [34], this source can ensure the absence of time delay relative to the start of the high-voltage pulse, the uniformity and low (few electron-volts) temperature of the plasma, the generation of ion beams with different mass compositions, and the operation in a frequency mode without reassembly. According to the experimental data [34], three triode operating modes are realized for different time delays τ_d: (i) a mode close to accelerator idle running ($\tau_d < 3$ μs); (ii) a growing-impedance mode ($\tau_d = 3-6$ μs), and (iii) a mode of sharp voltage drop, down to a short circuit ($\tau_d > 6$ μs). The existence of the three modes is attributable to various concentrations of the anode plasma produced beforehand. The respective plasma concentrations for the three modes were equal to $(2-5)\times 10^{12}$, $(3-6)\times 10^{13}$, and 10^{14} cm^{-3}.

In the experiments of Ref. [34], an ion beam containing three mass components (H^+, C^{n+}, and Cu^{n+}) was accelerated. Heavier ions were observed to emerge at the beginning of the anode current pulse. A comparison of the j_i/j_e^{ChL} ratios for different components of the ion beam revealed that the magnitude of the j_i/j_e^{ChL} increases with ion mass ($j_i/j_e^{ChL} = 9 \pm 2$ for H^+, and $j_i/j_e^{ChL} = 14$ for Cu^{n+}). The absolute values of the current density were equal to 40 A cm^{-2} for H^+, and 7 A cm^{-2} for copper ions.

The occurrence of a light hydrogen fraction in the HPIB composition can be explained by the high content of hydrogen in the dielectrics employed and the vacuum oils of accelerators. And since protons are least inertial, ion beams in real conditions (unless special precautions are taken) consist primarily of protons [35]. The employment of special materials and anode coatings makes it possible to obtain ions of heavier elements. In above-cited work [34], the anode was made of brass, hence the presence of copper ions in the HPIB. With the use of thin aluminum anodes in Ref. [17], Al^{2+} ions were accelerated to an energy of 3 MeV, the peak ion current being equal to 5 kA in this case. Golden and Kapetanakos [21] obtained deuteron beams ($E_i = 400$ keV, $I_i = 500$ A, $\tau = 50$ ns) with the use of aluminized mylar anode (6.25 μm) with a 25-μm thick CD_2 coating.

Experimental data suggest that the ion beams generated in RSs contain ions in lower charge states ($Z_i \leqslant 2$). The low degree of ionization is due to the low anode-plasma temperature (few electron-volts) and the low ion residence time in the cloud of oscillating electrons. The integral flux density of oscillating electrons does not typically exceed $10^{15}-10^{17}$ cm^{-2}, while the multiple ionization cross sections for atoms of different masses lie in the $10^{-18}-10^{-23}$-cm^2 range [36]. That is why the content of a highly charged component proves to be negligible in the ion beam.

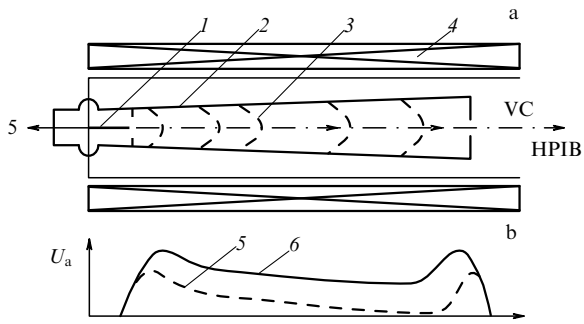

Figure 5. Schematics of a RT indented for the generation of HPIBs of multiply charged ions (a) and qualitative potential distribution along the anode axis (b): (*1*) cathode, (*2*) conic hollow anode, (*3*) oscillating electron beam, (*4*) solenoid; curves *5* and *6* correspond to the earlier and later instants of time [37].

Bystritskiĭ [37] proposed a modification of the electron-beam ion ionization technique by Donets [36] to generate multiply charged HPIBs in RSs. This idea is embodied in the system diagrammed schematically in Fig. 5. A characteristic feature of this system is a pointed cathode and a cone-shaped hollow anode. The ion source is the working gas kept under a pressure of $\sim 10^{-6}$ Torr in the system. An approximate relationship between the anode, relativistic electron beam (REB), and HPIB parameters in this system assumes the form

$$\ln \frac{R_{A_2}}{R_{A_1}} \geqslant \frac{m_i l^2 c}{\tau_{imp}^2 Z_i I_{lim}(1-f_e)}\,, \qquad (2)$$

where R_{A_2} and R_{A_1} are the radii of anode body bases, l is the body length, I_{lim} is the limiting REB current for the anode cavity, and f_e is the average charge neutralization degree. Calculations showed that a RT of this configuration with a neon working gas and the given parameters $\varphi_A = 500$ kV, $\tau_{imp} = 10$ μs, $B = 2$ T, $R_{A_1} = 10$ mm, $\alpha = 1°$ (the vertex angle of the anode cone), $r_C = 1$ mm (the radius of the cathode tip), and $l = 100$ cm generates the fraction of multiply charged ions with $Z_i = 8$, $E_i = 4$ MeV, and $I_i = 10$ A at a rate $n_i = 7\times 10^{13}$ particles per pulse. Providing 100% of the ions are extracted from the anode, the production efficiency of the multiply charged fraction in the system considered amounts to 1%.

So far we have considered works on the acceleration of positive ions in RSs. Bystritskiĭ et al. [38] conducted experiments on studying the production of negative H^- ions. These investigations were related to papers [39, 40] which reported that magnetically insulated diodes (MIDs) can produce H^- ion beams with $j_i \approx j_e^{ChL}$ (tens of A cm^{-2}), when the H^- content in the cathode plasma is high enough ($n_{H^-}/n_e = 0.05-0.1$). The experiments were run in a reflex tetrode to estimate the value of n_{H^-}/n_e. The 1 – 2-mm thick plates of CH_2 and $(CD_2)_n$ with a mesh of openings 1.6 mm in diameter, mounted on the cathode, served as the sources of H^- and D^-. For diagnostic purposes, advantage was taken of a double acceleration mode with an ion charge exchange in the anode. The H^- and D^- ions were emitted from the cathode due to explosive emission and were accelerated in the A – C gap. They then experienced charge exchange in the anode Dacron film with a surface density of 0.33 – 2.6 μg cm^{-2} and in the process lost a part of their energy. The ion beam was accelerated in the A – VC gap a second time and extracted for recording. To reject the ions accelerated from the anode

plasma, use was made of a series of grids placed within the A – VC gap, which were at the anode potential.

In this system, which was characterized by the following parameters $\varphi_A = 500-700$ kV, $\tau_{imp} = 80$ ns, and $B = 0.3$ T, it was possible to record H^- beams with $j_{H^-} = 0.4$ A cm^{-2} ($j_e^{ChL} = 10-25$ A cm^{-2}) and $n_{H^-} = 4 \times 10^{12}$ particles per pulse as well as D^- beams with $j_{D^-} = 4 \times 10^{-3}$ A cm^{-2} and $n_{D^-} = 4.4 \times 10^{10}$ particles per pulse. The estimated content of the negative ions in the near-cathode plasma proved to be very low (0.5 – 2% for H^-, and 4×10^{-2}% for D^-). The results obtained allowed a conclusion that H^- ions originated primarily from oil vapor adhered to the cathode surface, and that the H^- yield depended only slightly on the cathode material itself. The authors attributed such a significant disagreement with the data of Refs [39, 40] to the difference in the H^- production conditions in the plasmas, which invites further investigation.

2.4 Application of RSs

The use of HPIBs for the production of field-reversing proton layers and rings was proposed in the 1970s. The field-reversing layers and rings of high-energy charged particles provide an ideal configuration for the confinement of fusion plasmas. Since this furnished an opportunity to obtain high-precision REBs, attention was initially focused on the production and study of the properties of field-reversing electron layers [41, 42]. However, it was revealed experimentally that the synchrotron radiation of fast electrons would severely limit the dimensions of a thermonuclear reactor. To avoid radiation losses, proposals were made to replace high-energy electrons with protons possessing an energy of several hundred megaelectron-volts. That was precisely the time when Humphries et al. [6] reported the feasibility of multi-ampere proton beam production in RSs. Sudan and Ott [43] suggested a nuclear fusion device wherein an intense ion ring experiences magnetic compression with increasing energy to several hundred megaelectron-volts.

The first experiments on the application of RSs within the program of ion ring production were carried out by the group of Kapetanakos [44, 45]. An annular ion beam with the parameters $I_p \geqslant 200$ kA, $E_p = 0.6-1.2$ MeV, $j_p \geqslant 1$ kA cm^{-2}, $\tau = 55$ ns, and $\alpha \geqslant 4°$ was obtained in a ring RT-based system. The rotation of the intense annular ion beam was effected in its passage through a magnetic cusp.

Clauser [46] came up with the idea of using an HPIB as the energy source for nuclear fusion with inertial plasma confinement. For these purposes, Kawata et al. [47] developed and calculated in the one-dimensional geometry the scheme of a spherical RT (Fig. 6). In this system, use is made of the energy of an ion beam which is extracted towards the VC and arrives at the spherical target located in the central part of the structure. On the basis of Poisson equations, an expression was derived for the ion current density in this structure. The time dependence of the ion-beam energy flux at the target surface, required for the optimal target explosion, was also calculated. These calculations were done with the inclusion of electron collisions with the anode.

Bystritskiĭ et al. [48] investigated a new design for plasma-erosion interrupter (PEI) on the base of a plasma-filled RS involving the transition between two RS modes. The principle of operation of this scheme reduces to the accumulation — in the high-current mode of the plasma-filled RS — of a heavy current in the circuit and its fast termination when the RS switches to the high-impedance reflex tetrode mode. The

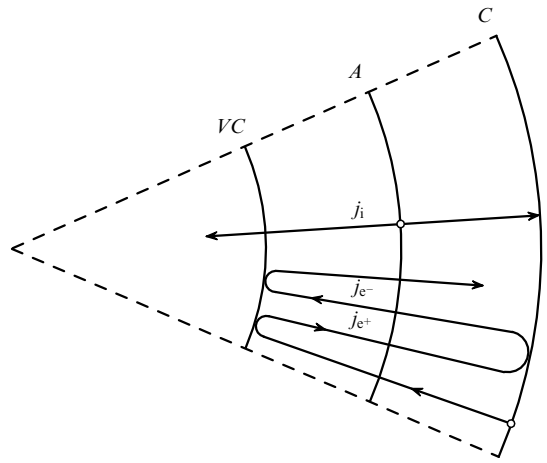

Figure 6. Schematics of a spherical RT [47].

experiments conducted demonstrated that the RSs in the PEI mode hold much promise for applications at a power level of about 10 GW.

Since this section is concerned with the applications of RSs, it is pertinent to note that the RSs are profitably used to generate high-power microwave radiation. The microwave radiation arises due to electron vibration in the potential well between the cathode and the VC as well as due to the oscillation of the VC itself. The power level of microwave radiation in RT type generators ranges up to several gigawatts [49 – 53].

By now the investigations of RSs intended for collective ion acceleration have been practically terminated. This is supposedly due to the fact that the oscillating VC is, on the average, immobile, and therefore the total acceleration path is not long even for a high acceleration rate. However, a series of papers [54, 55] saw the light recently, wherein an investigation was made into the effect of some technical problems (gas release, ion exit angle, microwave generation) on the collective ion acceleration.

3. Collective ion acceleration by a high-current REB in a neutral gas

The acceleration of ions in the injection of a high-current REB into a neutral gas was first discovered by Uglum and Graybill [56] in 1968. Protons with an energy $E_p \leqslant 5$ MeV numbering $n_p \approx 10^{13}$ particles per pulse were recorded in the experiments for the following parameters of the electron beam: $E = 1.5$ MeV, $I = 40$ kA, and $\tau = 25$ ns. The gas pressure was 0.15 Torr.

There occurred a possibility to develop a new ion acceleration technique as an alternative to the electron ring technique [5]. The new line of investigation attracted the attention of many researches and came to be developed vigorously. Many experiments were staged in a period of only a few years, which were performed by independent American laboratories [57 – 63]. Somewhat later, Russian scientists also joined this research [64 – 66].

Unlike many techniques whose development involved careful preparatory theoretical investigations preceding their practical implementation, this avenue of research began with experiments, and the theoretical models were advanced only later, starting from the experimental data gained in the experiments. It is noteworthy that none of

them acquired the form of a full-blown theory. In this connection, in Section 3.1 we outline the main results of experimental research, then in Section 3.2 we pass on to the discussion of the mechanisms responsible for the ion acceleration in gas and compare the theoretical models and calculated results with the experimental data. In Section 3.3 we discuss the ways of raising the ion energy by lengthening the period of synchronization between the ions under acceleration and the moving VC.

3.1 Main experimental results

The experimental layout depicted in Fig. 7 is typical for all the works described below. A heavy-current REB is injected through the thin anode of a field-emission diode into the drift chamber which is ordinarily of the form of a hollow cylinder with conducting walls. The chamber is filled with a gas (a gas mixture) at a pressure of 0.01 – 1 Torr. In the drift chamber there occurs ion acceleration by the electron beam, following which the electron and ion streams are separated and the ion beam arrives at the diagnostic region.

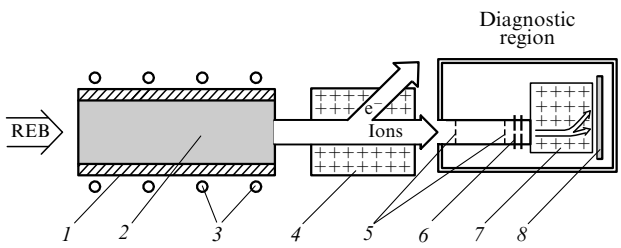

Figure 7. Schematic layout of the experiments on high-current REB-assisted ion acceleration in a gas: (*1*) drift chamber, (*2*) gas, (*3*) Rogowski loops, (*4*) deflecting magnet, (*5*) time-of-flight spectrometer, (*6*) collimators, (*7*) analyzing magnet, (*8*) nuclear emulsion specimen.

The diagnostic region comprises several sections: the section of time-of-flight diagnostics, the section of magnetic spectrometry, and lastly the specimens of nuclear emulsions. These diagnostic tools taken together enable the experimenter to gain complete information about an individual particle (its sort, charge, and energy). In addition to the main diagnostic tools, advantage is also taken of some other detection techniques. The maximum ion energy is determined by the absorption filter technique. To record currents in the system, use is made of the Rogowski loops, Faraday cups, and collector plates. The number of particles accelerated in an individual pulse is usually estimated from the radioactive level induced by the particles in a special specimen. To this end, the threshold nuclear reactions of the A(X, n)B type are employed, where A and B are the initial and final nuclei, X is the accelerated particle, and n are the neutrons produced due to the reaction. This technique makes it also possible to determine the particle energies, for the nuclear reaction thresholds are generally well known.

The experimental works of the 1970s were discussed in detail in the reviews [67, 68], while the data of new papers, as a rule, replicate the previously obtained materials. That is why we restrict ourselves to the presentation of the main data from Refs [67, 68], which are collected in Table 1.

We will formulate the main results of the experimental research in the form of propositions. Notice that not all of the phenomena listed below manifested themselves in every work. Furthermore, some of the research reports bear mutually exclusive information. This is characteristic of the earlier papers, when the then accumulated material was insufficient for the correct treatment of the observed phenomena. Here are the basic propositions:

Table 1. Experimental findings [67].

Ion	E_i, MeV	Z_i	I_i, kA	τ_i, ns
H	5 – 7	1	200	3
D	4 – 7	1	100	4
He	8 – 9	2	20	15
N	17 – 24	4 – 6	15	15
Ar	8 – 14	6 – 12	1 – 2	20

(1) Ion acceleration takes place only when the electron beam current I exceeds the limiting value $I_{\rm lim}$ corresponding to the passage of a longitudinally magnetized beam of radius a_0 through a conducting tube of radius R. This effect was present in all the works. The limiting current in them was calculated by the Bogdankevich – Rukhadze formula [69]

$$I_{\rm lim} = \frac{mc^3}{e}\,\frac{(\gamma^{2/3}-1)^{3/2}}{1+2\ln(R/a_0)}\,. \tag{3}$$

(2) The intensity of accelerating fields in all experimental works ranges from one tenth to several megaelectron-volts per centimeter.

(3) Accelerated ions are observed in a specific pressure range: $p = 0.01 - 1$ Torr. For every sort of gas there exists an optimal pressure $p_{\rm opt}$ whereby the number of accelerated ions is maximum (Fig. 8). The energy of accelerated ions increases with increasing pressure. This fact is characteristic of the majority of experiments. However, the pressure dependence of the energy of some sorts of the ions was not observed in several papers [58, 65]. This is supposedly due to the narrow pressure range under consideration in combination with insufficient sensitivity of the instrumentation equipment. Since the number of accelerated particles drops sharply with increasing pressure, the accelerated ions simply might have escaped detection.

(4) Not only the light ions of hydrogen and deuterium, but also heavier ions of other elements can be accelerated, depending on the sort of gas filling the drift chamber. The ions of helium, nitrogen, carbon, etc. were accelerated in some works [56, 58, 60, 65].

Different sorts of ions (for instance, He^+, He^{2+}, $N^{3+} - N^{6+}$ [58] or O^+, O^{2+}, $C^+ - C^{3+}$ [61]) can be accelerated in one and the same bunch. The energy of accelerated ions is

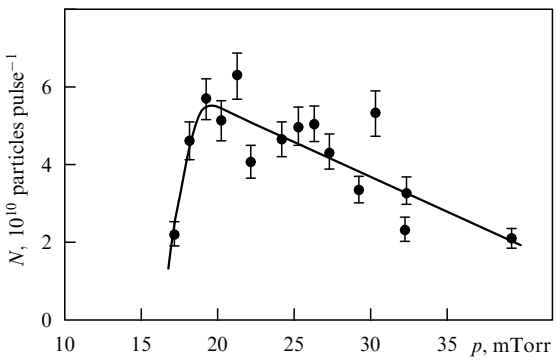

Figure 8. Number of accelerated ions as a function of nitrogen pressure in the drift tube [65].

Table 2. Parameters of an accelerated ion bunch in the electron beam injection into different gases.

REB energy, MeV	REB current, kA	REB pulse duration, ns	Gas	Pressure, Torr	Ion energy, MeV nucleon^{-1}	Number of ions, particles per pulse	Ion pulse duration, ns	Length of acceleration region, cm	Accelerating field, MV cm^{-1}	Ref.
1.5	40	50	H_2	0.05 – 0.2	5.0	10^{13}	3.0	30	0.2	[56]
			D_2	0.05 – 0.3			5.0			
1.0	160	80	H_2	0.2	1.5 – 3	10^{12}	—	10	0.2 – 0.3	[57]
			N_2	0.01 – 0.065						
1.0	115	50	H_2	0.15 – 0.65	12	$(0.5-2) \times 10^{12}$	5 – 10	10	1	[60]
1.5 – 2.0	50 – 100	90	H_2	0.2	1 – 5	$10^{11} - 10^{12}$	—	6.0	1	[61]
			D_2	0.2	1 – 5	$10^{11} - 10^{12}$	—	6.0	1	[61]
2	15	45	D_2	0.05 – 0.6	1.5 – 2.5	—	—	25	0.1	[62]
2.4 – 5.6	42 – 88	80	H_2	0.02 – 0.3	5 – 10	4×10^{14}	—	—	—	[63]
			D_2	0.02 – 0.3	5 – 10	4×10^{14}	—	—	—	[63]
0.65	20	50	H_2	0.05 – 0.4	1 – 3	10^{12}	5 – 10	30	0.1	[64]
			D_2	0.05 – 0.3			10 – 15			
0.7 – 1.1	20 – 48	50	H_2	0.02 – 0.3	2.5 – 3.5	$(2-7) \times 10^{10}$	10 – 35	30 – 60	0.1	[65]
			N_2	0.02 – 0.04						
0.33	6 – 30	80	H_2	0.01 – 0.3	0.2 – 0.5	$(1-3) \times 10^{10}$	—	—	—	[66]
1.3	50	50	H_2	0.075 – 0.6	2 – 4.5	10^{13}	20	15	0.1 – 0.3	[85]†

† The experiments of Ref. [85] were performed in the presence of an external magnetic field with $B = 0.8$ kG.

mass-independent and proportional to the ion charge, all experimental conditions being the same (Table 2). The record magnitude of the ion energy was attained in Ref. [60] for N^{7+} and is 29 MeV. Meanwhile, the intensity of the ion pulse for heavy gases (helium, nitrogen, etc.) is significantly lower than for hydrogen, which is clearly demonstrated by the data from Table 2.

(5) One or two accelerated-ion pulses can be observed in a single run, the ion energy in the first pulse exceeding the energy of the beam electrons several-fold (up to a factor of ten). The second pulse is typically lower in amplitude and follows the first pulse with some time delay. The double ion bunches were observed only in Refs [60, 65].

(6) The ion beam travels with a velocity approximately equal to that of the REB. In some works, the accelerated-ion pulse was observed to lag behind the leading edge of the REB.

(7) The ion pulse duration is an order of magnitude shorter than the electron pulse duration and it increases with ion mass (see Table 2).

(8) The acceleration region is localized near the anode and its dimension is of the order of the chamber diameter.

As noted in the review [67], initially the dependence of ion energy on the beam or medium parameters was extremely hard to estimate, because all the experiments were staged in various geometries and under different values of the electron current and energy.

The need to conduct comparable investigations for enhancing the predictability and improving the results of experiments was realized somewhat later. The mid-1970s saw the publication of the papers by Bystritskiĭ et al. [65] and also by Straw and Miller [62], wherein a study was made of the effect of electron beam-to-limiting current ratio $I/I_{\rm lim}$ on the ion energy. The $I/I_{\rm lim}$ ratio was varied by changing the ratio between the chamber radius R and the electron beam radius a_0. The investigations revealed that the energy of accelerated ions rises with increasing $I/I_{\rm lim}$.

More recently, Bystritskiĭ et al. [66] conducted a complex investigation by combining experiments with computational and theoretical work. As a result, the optimal gas pressure and the upper pressure bound were found to shift towards higher values with increasing $I/I_{\rm lim}$, all other factors being the same. In this case, the pressure range wherein ions are accelerated expands, this range expanding primarily upwards for a higher REB duration.

The authors' calculations showed that a simple fulfillment of the condition $I \cong I_{\rm lim}$ is not sufficient for ion acceleration to occur. There exists a threshold value of $(I/I_{\rm lim})_{\rm th}$ which marks the onset of ion acceleration. As the electron energy increases, the $(I/I_{\rm lim})_{\rm th}$ ratio decreases and in doing this varies over a wide range. General expressions for the threshold values of electron current in relation to the total set of parameters of the REB, the drift space, and the gas were also derived. Particular expressions valid in some special cases of practical significance were given. An analysis of these expressions revealed good agreement with experimental data gleaned in the greater part of the papers.

3.2 Theoretical models and evaluations, their comparison with the experimental data

The REB propagation in a gas is a rather complicated process. It is attended with such effects as ionization by primary and secondary electrons and ions, recombination, avalanche processes, etc. The beam propagates not only in the longitudinal direction, but in the transverse direction as well (expansion due to intrinsic spatial charge, and compression under the action of ions being produced). The many-sided nature of the effects under observation hampers the construction of a comprehensive theoretical model for the description of the totality of the occurring processes. As already noted, none of the models assumed the form of a full-blown theory.

Nonetheless, many models were posed. When considering the early stage of development of this line of research, mention should be made of the models due to Rostoker [70, 71] (the one-dimensional model of a traveling potential well), Wachtel and Eastlund [72] (ion acceleration by inverse Cherenkov radiation), Putnam [73, 74] (ion acceleration in the pinching of the REB), Uglum et al. [75] (acceleration at the breakdown front), Khodataev and Tsytovich [76] (ion acceleration in the focusing instability), etc. Of all the above-listed models, worthy of special consideration are the Rostoker model [70] which gives preference to the mechanism of ion acceleration due to the longitudinal beam deformation, and the model by Putnam [74] who believed the transverse beam deformation to be the main cause of ion acceleration.

Let us consider the mechanisms engaged in each of the models and compare the resultant concepts with the experimental data obtained using a longitudinal magnetic field.

The simple Rostoker model, which was also considered by Rosinskiĭ et al. [77], was subsequently complemented to acquire a complete form several years later. Alexander et al. [78] made a contribution of their own to the development of this model by including the effect of accelerated ions on the beam front dynamics. Kucherov and Kurilko [79] also made a contribution by mounting an effort to go over from a one-dimensional model to the two-dimensional one. The concluding stage in the development of the model of a traveling potential well is due to C Olson who performed, together with Poukey [80], a two-dimensional numerical simulation of the process and originated the concept of ion acceleration by a REB in a gas [81]. At present this model is referred to as the Olson model, sometimes with an addition of Rostoker's name.

The heart of the model is as follows. When a high-current REB carrying a current I greater than I_{lim} is injected into a chamber filled with the gas under a specific pressure, in the chamber near the anode there forms a VC, which is a potential well with a depth of about $1-1.5E$ [68]. It is well known that a VC is characterized by a high electron density and a low electron velocity. These conditions favor intensive gas ionization near the VC. In this case, the VC is saturated with gas ions, there occurs its charge neutralization, and it shifts along the chamber following the direction of motion of transit electrons. In the new position there also occurs gas ionization and the subsequent displacement of the VC. Therefore, a directed motion of the VC is formed, and a part of the ions can be involved in the accelerating process. The energy gained by the ions depends on the time during which the ions travel synchronously with the potential well. Long-duration synchronization is very hard to accomplish, and therefore attempts to accelerate ions to substantial energies (hundreds of megaelectron-volts) have not met with success. By now several approaches have been proposed to improve synchronization, and their future study would supposedly permit the researchers to produce ions with the desired energy. These approaches are outlined below.

Putnam's model deals with the motion of a local waist along the beam [74]. Its formation is explained as follows. If it is assumed that at some site in the electron beam there exists an ion bunch whose density is significantly higher than the ion density in the remaining part of the beam, the overcompensation condition should be fulfilled for radial forces in the beam at the site of bunch location. The so-called waist (the region of electron beam pinching) is formed immediately in front of the bunch. As a consequence, the electron density increases in this region, resulting in the production of longitudinal electrostatic field. Under a fast beam compression, the variation of inductance results in the production of a longitudinal induced field as well. These fields decelerate the electrons which find themselves in the waist region, and accelerate the ions, grouping them in the longitudinal direction. The motion of ion bunch in its turn results in the displacement of the pinching region, thereby effecting the synchronization between the ion motion and the fields involved in the accelerating process.

Among the significant disadvantages of this model is the fact that it does not take into account the real conditions of electron beam propagation through a gas and the dynamics of ion accumulation, with the consequence that the model is only qualitative. A more sophisticated model covering a transverse acceleration mechanism was elaborated by Gapanovich et al. [82] in 1978, who took into account the above-listed factors.

Both models built around the longitudinal and transverse acceleration mechanisms, which are used to advantage in interpreting several effects, nevertheless contradicted some of the experimental data. This led to the initiation of a new research cycle with a longitudinal external magnetic field, whose authors sought to confirm or refute a particular theory.

It was initially believed that the longitudinal magnetic field should suppress the nonadiabatic beam compression but should have no effect on the motion of the beam front. In the first experiments performed by Ecker et al. [60], the results were obtained which count in favor of the transverse acceleration mechanism. Strong external magnetic fields (3–10 kG) were found to completely suppress the ion acceleration. Moderate fields (250–500 G) did not suppress acceleration in all cases: protons were observed with the same energy as without the magnetic field, but with a flux lower by two–three orders of magnitude. A 100-G field had no effect on the accelerating process.

C Olson made an attempt to disprove the conclusions drawn from the data of the experiments conducted. Relying on numerical calculations he showed that a longitudinal magnetic field should also disrupt the ion acceleration induced by a traveling potential well [80]. He substantiated this statement as follows: on setting up the longitudinal magnetic field there always exist transit electrons which ionize the gas along the full length of the drift tube, thereby neutralizing the VC very quickly, which in turn makes the ion acceleration impossible.

However, attempts to reconcile the theory with the experimental data of Ref. [60] proved to be premature, because subsequent investigations [83–85] led to the opposite results. In the presence of the longitudinal magnetic field (7–15 kG) Straw et al. [83] used an electron beam ($E = 300$ keV, $I = 20$ kA, and $\tau = 100$ ns) to accelerate ions up to $E_{\text{i}} = 1.8$ MeV. Mako and Fisher [84] observed ion acceleration in a strong uniform magnetic field amounting to 8 kG. In this case, the average number of ions per pulse was two orders of magnitude lower than without the magnetic field. It is conceivable that Ecker et al. [60] failed to detect the accelerated ions for the reason of flux lowering. Roberson et al. [85] achieved positive results on ion acceleration by the electron beam ($E = 1.3$ MeV, $I = 50$ kA) in a strongly nonuniform field of acute-angled geometry. In this case, a conclusion was drawn on the basis of experiments conducted that a localized pinch cannot fulfil the function of the acceleration mechanism.

The resultant data compelled reconsidering the behavior of the Olson model in the presence of the longitudinal magnetic field. Kolomenskiĭ and Novitskiĭ [86] undertook a numerical simulation of the injection and propagation of the electron beam in the gas under the condition of longitudinal beam magnetization. They investigated a two-dimensional electrostatic model self-consistent with the ion motion. An indisputable virtue of the model was the treatment of the drift chamber as a cylinder with conducting walls. This approach gives stronger grounds to compare the data obtained by simulations with the experimental findings. The calculations done showed that a traveling wave of electric field with an intensity sufficient to accelerate ions to an energy much

higher than the initial energy of the beam electrons is formed in the drift tube.

Therefore, experimental and theoretical works with participation of a longitudinal external magnetic field confirm the Olson model and cast doubt on the mechanism of transverse ion acceleration.

Other experimental data also contradict the localized-pinch model. In particular, the ion acceleration by a beam with a characteristic parameter $v/\gamma \ll 1$ can hardly be attributed to this mechanism, for this condition is inconsistent with the nonadiabatic beam compression.

In the 1970s, obvious preference was given to the conception of transverse ion acceleration mechanism [67, 68] despite the fact that this model is in compelling contradiction with some of the experimental data. The cause may lie with the fact that the localized-pinch model, unlike the model of a traveling potential well, at that time was able to afford a qualitative explanation of such experimental facts as the acceleration of two or more ion bunches, the acceleration and production of a bunch behind the beam front, the upset of the accelerating process, etc.

These effects were theoretically substantiated on the basis of a traveling VC mechanism by Khodataev and Shakhanova [87] only in 1987. They considered the injection of a high-current REB into a gas with a uniform distribution of its number density C_v on the basis of a one-dimensional transient kinetic model. The authors distinguished three qualitatively different system operation modes; the heart of the problem is represented by the pictures in Fig. 9 obtained by numerical simulations using macroparticle approach.

At low gas pressures (Fig. 9a), the VC is produced near the injection plane. The number of ionized particles falls short of its charge neutralization, and therefore the VC remains at its production site. An insignificant part of ions accelerates in the VC region to be dumped into the drift space. The highest acceleration energy in this mode is equal to the injection energy E of the electron beam. This mode allows explanation of the existence of the lower pressure bound p_l. The ion acceleration is not observed for $p < p_l$.

As the gas pressure increases, the build-up of ionization and ion accumulation rate in the VC region become sufficient for the realization of a traveling VC mode. The traveling VC structure is produced each time the medium is capable of compensating for the volume charge of the beam. This is also confirmed by other works on the numerical simulation of the REB injection into a fully ionized plasma [88], a conducting nonscattering medium [89], and a gas [90, 91].

At moderate pressures (Fig. 9b), two groups of ions undergoing acceleration are formed, one of which is ahead of the beam front and the other travels behind the beam front. Calculations showed that the ions of the first group acquire energies of the order of $2m_i V_{VC}^2$, where V_{VC} is the velocity of the VC motion, and their fraction amounts to $(1 - m_i V_{VC}^2/2E)$ of the total number. The ions of the second group are accelerated to energies lower than $m_i V_{VC}^2/2$, and their fraction is estimated at $m_i V_{VC}^2/2E$ of the total number.

Because $m_i V_{VC}^2/2E \to 1$, only one pulse of accelerated ions was recorded in the majority of experiments, which lagged behind the leading edge of the VC. The experimental detection of two accelerated-ion bunches in a single run [58, 65] is attributable to the fact that the number of ions in the first bunch proved to be high enough for their recording. This model adequately accounts for the occurrence of ion bunches relative to the VC front as well as the intensities of ion pulses.

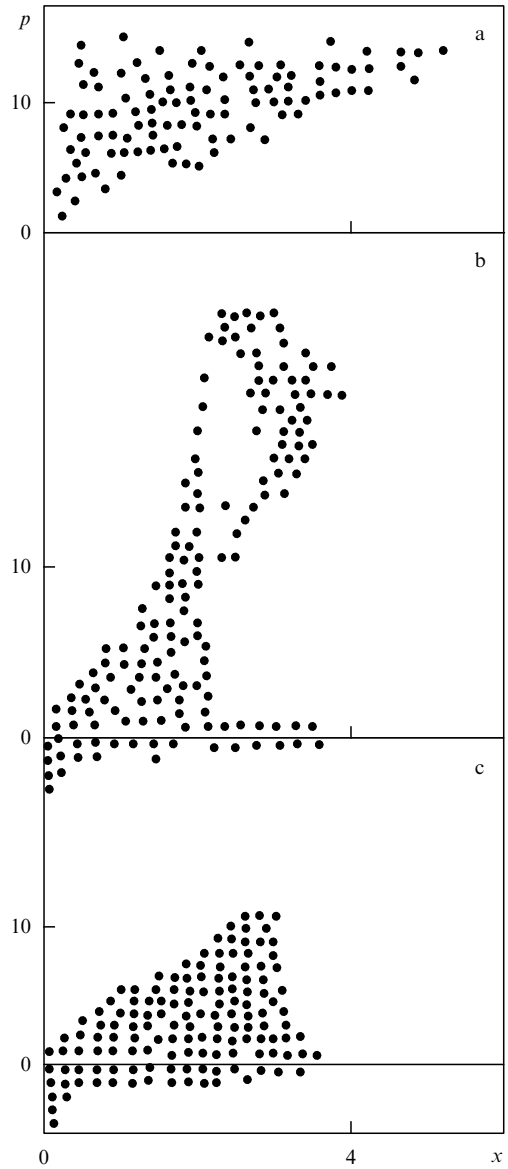

Figure 9. Ions phase portrait at different gas concentrations: (a) $C_v < 0.1$, (b) $0.1 < C_v < 1$, (c) $C_v > 1$ ($C_v = L/\lambda$, where λ is the number of ion–electron ionization pairs in a 1-cm path of an electron with an energy of 1 MeV, and L is the spatial scale unit) [87].

At higher gas pressures (Fig. 9c), the velocity of the traveling VC becomes too high. As a result, the momentum gained by the ions in its field proves to be insignificant. This mode accounts for the existence of the upper pressure bound p_u above which the ion acceleration is also not observed.

The above-discussed model explains the majority of experimental results and thereby allows a proposition that the mechanism of longitudinal beam deformation plays a leading part in ion acceleration by a high-current REB. It is conceivable that in some special cases account must be taken of the transverse acceleration mechanism as well.

3.3 Ways of synchronizing the motion of the VC front and the ions under acceleration

The ions involved in the accelerating process by a traveling VC initially move together with the potential well whose velocity will be denoted as V_{VC}. The ions gradually acquire velocities greater than V_{VC} to escape through the front wall of

the potential well. This terminates the accelerating process, and subsequently the ions merely drift along the chamber.

In uncontrollable processes, the synchronization of the VC motion with the ion motion exists for a short time, and therefore the path over which the acceleration occurs is no longer than the chamber diameter. This circumstance limits the accelerated-ion energy to several tens of megaelectron-volts. By lengthening the synchronization time it is possible to attain ion acceleration to hundreds of megaelectron-volts and even to 1 GeV.

The velocity of the VC motion is amenable to control. This can be attained in several ways. One of them relies on gas concentration variation along the beam path. In 1974 this dependence was experimentally borne out by Tkach et al. [92] who controlled the velocity of travel of the ionization front by producing a pressure gradient along the chamber axis. These experiments were staged with a REB ($E = 0.8$ MeV, $I = 25$ kA) injected into the different gases (hydrogen, helium, neon, argon, and air). The measurements showed that the pressure variation from 0.2 Torr at the beginning of the chamber to 1 – 2 Torr at its end caused the ionization front velocity to rise by a factor of 1.4 – 1.6, depending on the sort of gas.

In 1987, Khodataev and Shakhanova [87] employed a one-dimensional stationary kinetic model to derive the dependence of the velocity of travel of the potential well front on the gas density (Fig. 10), which was in qualitative agreement with the available experimental data.

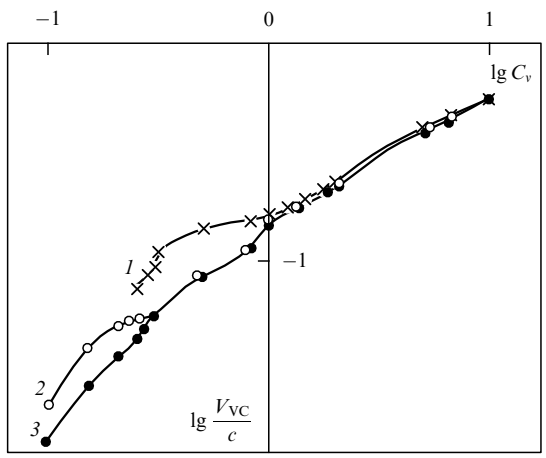

Figure 10. Relative velocity V_{VC}/c of the VC front, where c is the velocity of light, as a function of the gas density: (*1*) $M = 10^2$, (*2*) $M = 10^3$, (*3*) $M = 10^6$ (M is the reduced ion mass) [87].

The effect of gas concentration on the ion acceleration was experimentally investigated by Kolomenskiĭ et al. [64] in 1975. To this end, a two-section drift chamber was designed and fabricated, whose sections could bear different gases at different pressures. The highest ion energy was experimentally established to increase, but the build up was not as significant as might be anticipated. This is supposedly due to the difficulties in selecting optimal parameters of the system (section lengths, gas pressure) required for a long-duration synchronization.

When selecting the spatial profile of gas concentration it should be borne in mind that the build up of VC travel velocity is saturated with increasing the gas density [93]. The practical realization of this way presents a real challenge, because it is quite difficult to produce the requisite spatial concentration distribution inside the drift tube.

A more simple way of controlling the velocity of traveling VC front is realized when employing an external ionizer. Olson et al. [94] proposed the application of a laser beam as the ionizer, whose programmed displacement should give the distance – time curve for motion of the ionization front. This is possible in circumstances when the beam electrons and the ions entrained by the accelerating field produce virtually no ionization of the working gas. This is the way proposed to accelerate ions up to relativistic energies.

When selecting the velocity of ionization front it should be taken into account that a REB may not have time to set up the structure of traveling VC as the velocity approaches the relativistic values. In this case, the ionization front would leave behind the VC front and further ion acceleration would terminate. The problem of determining the limiting velocity of the ionization front was taken up by Khodataev et al. [93]. According to their calculations, the VC front velocity for the optimal conductivity increases with decreasing current to attain a value of ~ 0.5 for $I = I_{\text{lim}}$. Therefore, the VC produced by a beam with an above-limiting current cannot travel with a relativistic velocity. These results agree with qualitative estimates made in Ref. [76] and are of importance in selecting the experimental conditions.

Experiments demonstrating the possibility to control collective ion acceleration with the aid of an external ionizer were conducted by Olson et al. [95] in 1985. The electron beam ($E = 1$ MeV, $I = 30$ kA, $\tau = 40$ ns, and $a_0 = 1$ cm) was injected into 30-cm long metal drift tube with an internal radius of 1.1 cm filled with a gas at moderate pressure. In this case, the gas pressure was selected as low as possible to significantly reduce the beam-induced ionization. Upon formation of the VC, a laser beam was admitted to the chamber through a special transparent window. The beam power was selected in such a way as to produce the plasma with an ion density high enough to neutralize the VC. The neutralization time of the next stationary VC state due was varied by changing the laser beam intensity, making it possible to rise the travel velocity of the potential well.

The experiments showed that ions in a system with an external ionizer can be entrained and accelerated by the VC in the programmed phase velocity mode. In this case, the accelerating fields ranged up to 0.33 MV cm^{-1} over a length of 30 cm.

The data obtained for H^+, D^+, and He^{2+} ions are shown in Fig. 11 in comparison with the results produced with a system without an external ionizer (EI), all other factors being the same. The working gases selected for H^+, D^+, and He^{2+} ion acceleration in the experiments with an EI were Cs (0.05 Torr) and H_2 (0.05 Torr), Cs (0.05 Torr) and D_2 (0.05 Torr), Cs (0.05 Torr) and He (0.05 Torr), respectively. In the experiments without the EI, the respective working gases were H_2 (0.1 Torr), D_2 (0.1 Torr), and He (0.1 Torr).

The advantage of employing an EI to substantially rise the ion energy is evident. The energy of accelerated ions in experiments with a laser ionizer is 5 – 10 times the energy obtained in the ordinary way. In this case, the acceleration margin is large ($\beta = 0.1$), for the authors did not pursue the goal of maximizing the ion acceleration. They merely demonstrated the promise of this acceleration technique by considering its initial stage only.

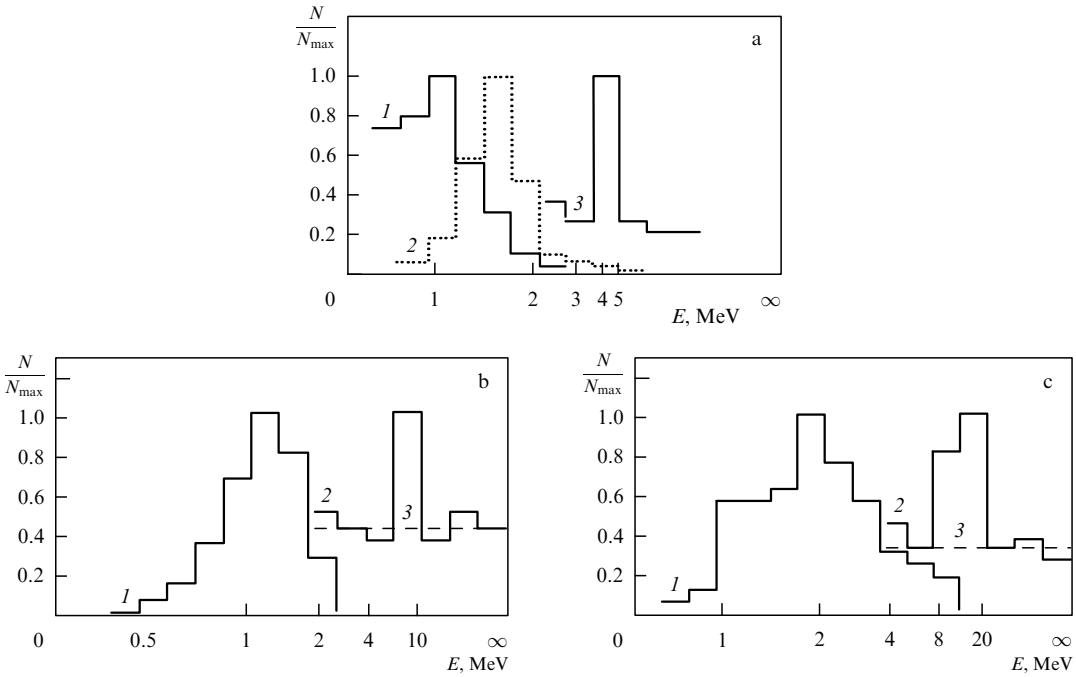

Figure 11. Accelerated-ion energy distribution for H^+ (a), D^+ (b), and He^{2+} (c) [85]: (*1*) natural process without an EI; (*2*, *3*) the process with an EI, the respective lengths of the drift tubes being 10 and 30 cm.

4. Collective ion acceleration in a Luce diode with an insulated anode

4.1 Main experimental findings and conceptions of the acceleration mechanism

One more scheme of collective field acceleration of positive ions was proposed in 1973 [96]. Its elaboration was pursued by J Luce and his collaborators at the Lawrence Livermore National Laboratory. The systems for collective ion field acceleration realized by that time were divided into three main categories: vacuum diodes [97], plasma diodes [98, 99], and drift chambers filled with a moderate-pressure neutral gas [56]. The new device which combined the diode gap and the drift region could not be placed into any of the existing categories and was therefore described by Luce as a pulsed accelerator operating in a vacuum. This kind of device later came to be known as the Luce diode.

In a Luce diode (Fig. 12), the proper diode region is represented by the cathode, usually shaped into a rod with a pointed end, and a compound anode with an axially symmetric opening at the center. The cathode apex can be made of graphite, quartz, copper, tungsten, aluminum, and other materials. The graphite cathode was experimentally found to be preferable to others because it produced a better collimated electron beam, thereby reducing the angle of divergence of the accelerated ions and electrons. A significant part of the experiments was therefore conducted using precisely the graphite cathode [96, 100 – 104]. The anode, which is the main supplier of ions, has a dielectric insert in the central part. The insert is made of materials which incorporate the sort of ions to be accelerated (natural polyethylene CH_2, deuterated polyethylene CD_2, caprolan, etc.). The anode is placed in a metal grounded structure made of brass [96], copper [100] or other materials, which serves the function of carrying away the reverse current. In modified Luce diodes, good use is also made of plasma anodes (PAs) [103, 104] and of anodes complemented with a small dielectric tube [102, 105].

The drift region is located immediately behind the diode region and is a cylindrical evacuated chamber approximately one meter long. Ion acceleration takes place primarily in the drift region, at the end of which there is a target for recording the electron – ion beam. The diagnostic complex comprises about the same set of tools that was described in Section 3.

When comparing the experimental results on the entire spectrum of accelerating schemes, the Luce diodes should be recognized as the most preferable. It is precisely the vacuum drift chambers with a dielectric anode that allowed the researchers to attain the greatest numbers and highest energies of the accelerated ions.

Luce et al. [96] reported the results of their work on the FX-75 accelerator. They obtained hydrogen and deuterium ions with an energy of 15 MeV in amounts of 10^{14} particles per

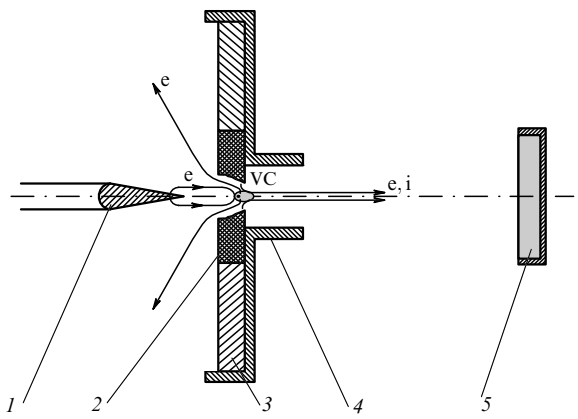

Figure 12. Schematic of the Luce diode for collective ion acceleration: (*1*) cathode, (*2*) plasma-producing dielectric (ion supplier), (*3*) anode, (*4*) drift tube, (*5*) detector of accelerated beams.

pulse for the following parameters of the electron beam: $E = 4$ MeV, $I = 30$ kA, $\tau = 30$ ns, and $v/\gamma = 0.3$ is the Budker parameter. The highest energy recorded was 45 MeV for protons, and 135 MeV for fluorine ions. Boyer et al. [106] reported recording protons with an energy up to 16 MeV ($U_0 = 1.5$ MV) and current regimes $I_i \geqslant 200$ A. With REB ($E = 1.5$ MeV, $I = 30$ kA, $\tau = 30$ ns) acceleration of heavier ions (N, Ne, Ar, Kr), Destler et al. [107] obtained ions with an energy of ~ 4.7 MeV nucleon^{-1}. The total energy of such ions, Kr for instance, was 390 MeV. Faĭnberg [108] communicated the acceleration of xenon ions up to 900 MeV.

In the majority of papers, the processes occurring in Luce diodes are described as follows. Initially, an uncompressed electron beam produces an avalanche breakdown of the anode material on the diode side. A dense anode plasma with a number density of $\sim 10^{18}$ ion cm^{-3} is created. The anode plasma leads to a reduction in electron space charge and a pinching of the electron beam towards the axial anode opening. During this process there arises a reverse current which travels radially until it reaches the anode grounding electrode. A part of ions accelerates together with the radial reverse current. However, because of the large energy spread these ions are of no practical significance. Another part of ions travels towards the VC produced in the anode region. The ion current density of this emission is given by

$$n_i \approx \frac{\varepsilon_0}{e}\frac{j_e}{j_c}\frac{U_{VC}}{d^2}(1+\alpha)^{1/2}\,, \tag{4}$$

where j_e/j_c is the ratio between the current density at the anode and the nonrelativistic current density, U_{VC} is the virtual cathode potential, d is the distance between the locations of the VC and the anode plasma, $\alpha = eU_0/2mc^2$, and U_0 is the anode voltage. For typical experimental parameters $U_0 = 3$ MV, $j_e/j_c = 1.4$, $U_{VC} = 6$ MV, and $d = 6$ cm, we obtain $n_i \approx 10^{13}$ ion cm^{-3}. On their way to the VC, the ions partially neutralize the space charge, allowing the beam front to travel away from the anode towards the drift region. In this way there originates motion of the VC at the front of the nonneutralized beam, which involves the ions in the accelerating process.

A hypothesis of this kind for the ion acceleration mechanism in Luce diodes was put forward and experimentally verified by Adamskiĭ and his associates in 1977. Much later, in 1989, a start was made on the theoretical investigations of ion acceleration in the stream of electrons with the VC in the absence of a neutral gas. Dolgopolov et al. [109] studied the acceleration of an ion bunch by the stream of electrons with the VC in the one-dimensional approximation, when the ion bunch was modelled by a charged plane. It is pertinent to note that the charged plane model is better suited to the description of acceleration of a single large charged particle rather than an ion bunch, where every ion experiences the fields of not only electrons and electrodes, but ions as well. However, the VC potential evolution arising from the appearance and motion of the ion bunch in the drift region was found to be capable of efficient ion accelerating even in the context of so crude, while self-consistent, a model of the ion bunch embedded in the electron stream.

Dolgopolov et al. [109] made a qualitative comparison of the data obtained by simulations and the experimental findings of Stepanenko et al. [110] from the Khar'kov Institute of Physics and Technology. The experiments were performed with the following REB parameters: $E = 1$ MeV, $I = 10$ kA. The investigation led to the production of a beam of carbon ions with an energy of 20–40 MeV (1.5–3 MeV nucleon^{-1}) and a current of 10–20 A. The comparison showed a good accord between the basic experimental and theoretical data. Also noted was the comparability of accelerated-ion energies predicted in the context of the model and those established experimentally.

Dolgopolov et al. [111] undertook a theoretical investigation of ion acceleration by the VC potential with the self-consistent inclusion of the action from the ion-induced fields. The analysis was based on the numerical solution of the system of the Vlasov–Poisson equations

$$\frac{\partial^2\varphi}{\partial\xi^2} = -ZQ\int_{-\infty}^{\infty} d\eta\, f + Q\begin{cases}\dfrac{2-j(\tau)}{(1+\varphi)^{1/2}} & \text{for } 0<\xi<\xi_m\,,\\[2ex] \dfrac{j(\tau)}{(1+\varphi)^{1/2}} & \text{for } \xi_m<\xi<1\,,\end{cases} \tag{5}$$

$$\frac{\partial f}{\partial\tau} + \eta\frac{\partial f}{\partial\xi} - \frac{Z}{2}\frac{\partial\varphi}{\partial\xi}\frac{\partial f}{\partial\eta} = 0\,, \tag{6}$$

where φ is the potential, f is the ion distribution function, j is the electron flux density, ξ, η, and τ are the normalized coordinate, velocity, and time, ξ_m is the coordinate of a VC position, and Q is the parameter proportional to the unperturbed electron density. The analytical solution to the system of equations (5) and (6) is of the form

$$\varphi(\xi,\tau) = \begin{cases} -1+\left(\dfrac{3}{4}\right)^{4/3}\left[Q\big(2-j(\tau)\big)\right]^{2/3}\left[\xi_m(\tau)-\xi\right]^{4/3} \\ \qquad \text{for } \xi<\xi_m\,,\\ -1+\left(\dfrac{3}{4}\right)^{4/3}\left[Qj(\tau)\right]^{2/3}\left[\xi-\xi_m(\tau)\right]^{4/3} \\ \qquad \text{for } \xi>\xi_m\,.\end{cases} \tag{7}$$

The numerical analysis of the solution (7) showed that the appearance of ions in the drift region may lead to the accelerated VC motion without a significant decrease of potential steepness (Fig. 13). This in turn serves to increase

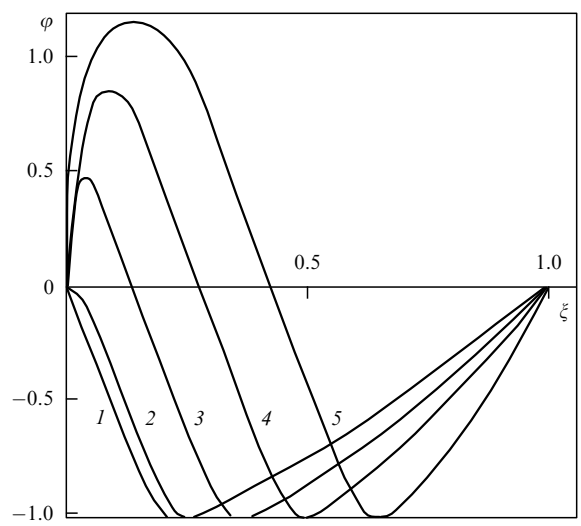

Figure 13. Potential as a function of coordinate at different points in time τ [111] ($\tau = tV_0/L$, where V_0 is the electron velocity in the injection plane): (*1*) $\tau = 0$, (*2*) $\tau = 0.049$, (*3*) $\tau = 0.098$, (*4*) $\tau = 0.147$, (*5*) $\tau = 0.195$.

the ion energy by about an order of magnitude in comparison with the electron energy. The highest energy gain is exhibited by the ions located closer to the bottom of the potential well, their number decreasing in this case.

In the experimental study of ion acceleration in the Luce diodes, Adler and Nation [112] also arrived at an initial conclusion that the ions are most likely accelerated due to the displacement of the potential well at the front of the non-neutralized beam. In the course of investigations they categorically disproved the assumption that the ions are accelerated in the deep stationary potential well, because they observed protons with an energy exceeding the electron injection energy by a factor of 10. In this case, the measured effective depth of the potential well at the beam front proved to be smaller than the diode voltage accelerating the electrons. The observation of protons and deuterons with an energy exceeding the energy of the protons in the same ion pulse was also an argument in favor of the acceleration mechanism at the beam front. In the experiments, use was made of an electron beam with the typical parameters $E = 0.4-1.1$ MeV and $I = 15-50$ kA.

At a later time, upon comprehensive investigations of the electron and ion beam propagation as well as of the ion energy spectrum, Adler et al. [113] drew a conclusion that the ion acceleration by the beam front cannot serve as the acceleration mechanism. The study of the ion energy spectrum and the time evolution of the accelerated beam underlay the reconsideration of the mode of thought. In the experiments, advantage was taken of the electron beam ($E = 500-700$ keV, $I = 65$ kA, $\tau = 100$ ns) injected through the opening (narrowed towards the end) in the polyethylene anode insert. The anode insert was approximately 1.2 cm in thickness, and the minimal diameter of the opening was 1.2 cm. The cathode made of aluminum had a conic apex whose minimal diameter was ~ 0.2 cm. For the most part these experimental examinations were made in a drift tube 7.3 cm in diameter, ranging from 60 to 150 cm in length.

The temporal analysis data on accelerated ions were obtained employing a Faraday cup with a copper foil stack spaced at 1 m from the anode. In these experiments electrons were deflected by the magnetic field so that the protons, when brought to rest in a specific foil, predetermined the current pulse from this foil. The signals recorded yielded the relative temporal resolution of the ion energy distribution. The temporal evolution of proton energy spectrum at the end of the 1-m long drift tube is displayed in Fig. 14. Reference to this figure shows clearly that the width of ion pulses decreases with an increase in the proton energy. Furthermore, the highest-energy protons ($E_i > 4.7$ MeV) emerge at the trailing edge of the diode pulse. The authors noted that these two simultaneous effects cannot be explained on the basis of the model of ion acceleration by the beam front, and therefore they rejected this model.

In search for an alternative model of ion acceleration in the Luce diodes, Adler et al. [113] proposed a wave acceleration mechanism. Having considered different wave interaction mechanisms which may be responsible for ion acceleration, the authors arrived at the conclusion that the mechanism involved supposedly is the electron – ion two-beam instability. It was noted that the conditions suitable for the development of this instability are much pronounced in a pulse. This process was first modelled by Godfrey and Thode [114] in 1975 for a beam with a small v/γ ratio. According to the modelling results, the ion energy peak was

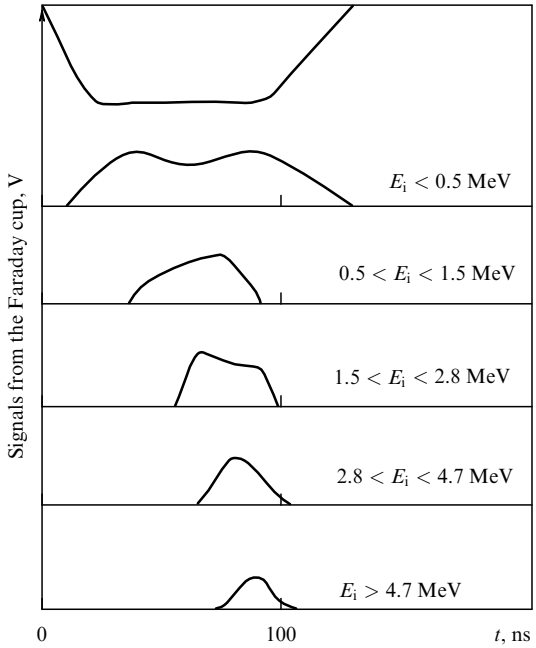

Figure 14. Temporal evolution of the proton energy spectrum at the end of the accelerating region [113].

approximately three times the beam electron energy. Davidson et al. [115] analyzed the linear stage of instability for a beam in a tube, subject to the condition that the beam radius is much smaller than the tube radius. A comparison of the wave parameters estimated by the formulae of Ref. [115] and those obtained experimentally in Ref. [116] revealed a minor quantitative discrepancy between the values of the parameters being compared, thus allowing the authors to become firmly convinced in their choice.

It is noteworthy that the experiments of Ref. [113] were performed with a beam characterized by a substantially longer pulse rise time ($\tau = 100$ ns) than in many other works ($\tau = 30-40$ ns) and were staged in a slightly different geometry. It is conceivable that these circumstances had affected the results of the experiments, in which the dominant role is played by the wave acceleration mechanism.

To improve the efficiency of ion acceleration in the Luce diode, an experimental study was made in Refs [100, 101, 116] concerning the effect of parameters of the accelerating system and the electron beam on the output parameters of the ion pulse.

Zorn et al. [100] investigated how additional 'floating' electrons introduced into the region behind the anode affected the acceleration efficiency. The data were more likely to be qualitative rather than quantitative in nature. The introduction of two additional electrodes was noted to result in a significant rise in ion energy (from 4 – 6 MeV to 8 – 16 MeV).

Hoeberling and Payton [116] studied the effect of injected-to-limiting current ratio $I/I_{\rm lim}$ on the ion acceleration in the drift tube. The limiting current magnitude was varied by changing the radius of the drift tube. The experiments showed that ions are accelerated in the drift tube only when $I/I_{\rm lim} > 1$, the acceleration efficiency rising with increasing the $I/I_{\rm lim}$ ratio. Employing the FX-25 accelerator ($E = 2.2$ MeV, $I = 23$ kA, $\tau = 40$ ns) they recorded the ions with an energy of 5.5 – 6.1 MeV at a maximum for $I/I_{\rm lim} = 1.6$. A moderate

ion activity was also observed for $I/I_{\rm lim} < 1$ at a distance of several millimeters from the anode, which is indicative of some initial ion acceleration occurring in the A – C gap or inside the opening. The acceleration in the A – C gap was originally discovered in work [117].

Bystritskiĭ et al. [101] investigated the effect of current pulse parameters, namely the rise time and the occurrence of a prepulse, on the acceleration efficiency. The experiments were conducted on the 'Tonus' accelerator ($E \approx 1$ MeV, $\tau = 50$ ns, $v/\gamma = 0.8$). The measurement data showed that the improvement of vacuum conditions, the suppression of charging prepulse, and going over to electron beams with significantly shorter rise times bring about a significant gain in accelerated-ion energy. In experiments with a caprolan insert which enabled the suppression of the prepulse and shortening of the current rise time the peak proton energy was $E_{\rm p} = 5$ MeV, and the total yield $n_{\rm p} = (1 \pm 0.3) \times 10^{13}$ particles pulse^{-1}. When operating without the caprolan insert, the ions were accelerated up to energies $1.9 \leqslant E_{\rm p} \leqslant 2.7$ MeV at a production rate $n_{\rm p} = (1 \pm 0.3) \times 10^{14}$ particles pulse^{-1}.

The current of accelerated ion beams depends significantly on the density of plasma produced in the electron beam injection or pre-produced (in some versions of the Luce diode). In particular, a plasma can be generated by high-power laser irradiation of the anode from the VC side. A plasma anode (PA) can also be used to advantage as the plasma source [103, 104].

We call attention to the fact that the problem of long-duration synchronous motion of the VC and the accelerated ions is as important in this case as in the ion acceleration in gases. It may be solved by taking advantage, for instance, of longitudinally nonuniform dielectric channels (Fig. 15) [118]. A scheme of this kind was experimentally tested in work [119] in which the number of accelerated ions for a conic dielectric element was shown to be substantially larger than for a cylindrical one. In relation to this idea, Dubinov and Kornilova [120] considered the problem of VC formation in a dielectric channel and showed that the VC formation time increases with an increase in the permittivity ε.

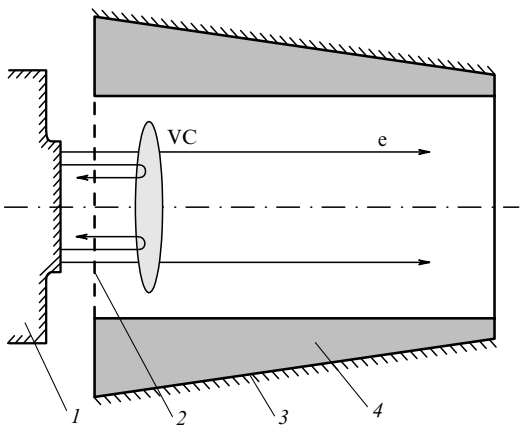

Figure 15. Schematic of the collective ion accelerator in a profiled dielectric channel [118]: (*1*) cathode, (*2*) anode mesh, (*3*) drift tube, (*4*) profiled dielectric channel.

4.2 Modifications of the Luce diode

Among the modified Luce diodes are the 'Kovcheg' electron accelerator with a PA [103, 104], developed and implemented by the staff members of the Russian Federal Nuclear Center (All-Russia Scientific Research Institute of Experimental Physics) in Sarov. Coaxial plasma injectors fitted with the nozzles requisite to ensure a plane plasma geometry in the anode region were selected for the PA creation. Nitrogen, krypton, and xenon were employed as the working plasma-producing gas. The highest plasma number density in the paraxial region was $\sim 10^{14}$ cm^{-3}. In experiments, use was made of a cathode in the form of graphite brushes in a circle 40 mm in diameter, which extended 20 – 50 mm above the metal disk of diameter 50 mm, or a graphite planar cathode 160 mm in diameter. The diode gap was 20 – 80 mm. The electron beam ($E = 200$ keV, $I = 30$ kA) was injected into the 1-m long drift chamber ~ 35 cm in diameter.

In the experimentation, measurements were made of the output current which proved to exceed the limiting vacuum current by more than an order of magnitude. This may be attributed to a partial neutralization of the space charge of transit electrons by plasma ions captured and accelerated by the virtual PA – VC diode. In this case, the difference signal of electron and ion currents was recorded. The ion beam parameters were not studied experimentally in this work, but computer simulations of ion acceleration were made in the configuration with parameters approximating the real experimental conditions.

The simulations were performed using an applied program package on the basis of the 2.5-dimensional PIC 'KARAT' code written by V Tarakanov and outlined in Ref. [121]. According to the calculations, it is possible to accelerate heavy-ion kiloampere beams to an energy of ~ 5 MeV nucleon^{-1}. An analysis of the phase portraits of an ensemble of particles allowed determination of the law of motion of the VC as a whole along with the law of motion of the front of the ion beam under acceleration. Both motions were found to occur approximately evenly, the ion beam front keeping slightly ahead of the VC. A similar result was obtained by Ginzburg et al. [88] with a one-dimensional numerical model for the electron injection with a super-limiting current into a moderately dense gas. An analysis of the evolution of the spatial ion distribution showed a good focusing of the trapped ion beam, which was emphasized in Refs [96, 101].

A vircator with a plasma anode was also theoretically investigated in Ref. [122] (primarily for the purposes of microwave generation). The REB modulation and the microwave radiation frequency were found to enhance with increasing ion number density. The REB modulation may prove to be advantageous also for collective acceleration [123].

Vijayan et al. [102] presented another modification of the Luce diode, wherein a dielectric tube attached to the anode on the side of the drift tube fulfilled the function of an ion source. For an electron beam ($E = 200$ keV, $I = 6$ kA) injection into vacuum in this geometry, the accelerated-ion energy was ~ 1 MeV for protons, ~ 15 MeV for carbon ions, and ~ 21 MeV for oxygen ions. The experiments were staged with a graphite planar cathode 5 cm in diameter and an anode in the form of a copper mesh with a transmittance of 60%. The A – C gap was 8 mm. The electron beam was injected through a dielectric tube of diameter 5 cm into a drift tube ~ 15 cm in diameter and about 1 m in length. The authors observed a strong dependence of the current on the length of the dielectric tube. The best results were obtained when the length of the dielectric tube was equal to the width of the VC potential well. A rapid attenuation of the propagating current

was observed for shorter lengths, which is associated with a low level of beam neutralization.

The technique of collective VC-assisted ion acceleration in systems with the ion production at the anode (conventional and modified Luce diodes) holds the greatest promise today and is being vigorously investigated. As an example, we mention the two-stage ion accelerator elaborated in the Khar'kov Institute of Physics and Technology [124]. In the first stage of this accelerator there occurs ion acceleration and the VC-assisted modulation of the ion current. The second stage involves finish accelerating of the ions in their interaction with the electrodynamic structure.

5. Other techniques of collective ion acceleration in systems with a VC

5.1 Collective ion acceleration in a vacuum spark discharge

The acceleration of ions in a vacuum spark discharge was discovered by A Plyutto in 1960 [98, 99]. The schematic diagram of the experiment on the production of ion and electron beams from vacuum spark plasmas is given in Fig. 16. The spark source generates the plasma which enters the accelerating gap through an emission opening. A variable or d.c. voltage is applied across the gap to accelerate electrons towards an electrode *1*. High-energy protons with $E_p = 4-5$ MeV at a production rate $n_p = 10^{11}-10^{12}$ particles pulse^{-1} and carbon ions with $E_i = 15-20$ MeV were recorded in the cavity of the electrode *1*, the voltage applied across the gap amounting to 200 – 300 kV.

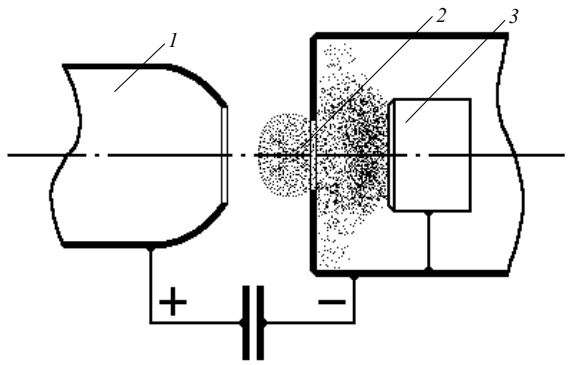

Figure 16. Schematics of the experiment on ion acceleration in a vacuum spark discharge: (*1*) hollow electrode, (*2*) plasma emission opening, (*3*) spark source [99].

More recently, Plyutto's group undertook a series of investigations of this phenomenon to establish the common immanent features of the processes accompanying the beam acceleration in a vacuum spark discharge [97, 125, 126]. Summarizing the results obtained, we note the following:

(i) the peak ion energies can exceed the voltage applied across the gap by a factor of 10 – 100; in this case, the ions travel in the direction of electron beam propagation, in opposition to the externally applied potential difference;

(ii) the intensities of internal accelerating fields can be as strong as 10^5-10^6 V cm^{-1};

(iii) the highest ion energy is proportional to the ion charge multiplicity ($\sim 3ZeU_0$);

(iv) the ions are accelerated only in the unstable mode of a vacuum spark, which is characterized by sharp current density surges and is attended with a significant increase in the density of electron beam along the direction of ion acceleration.

Items (i) – (iv) allowed a conclusion that the acceleration of positive ions takes place under strong collective interactions of the electron beam with plasma ions. Several mechanisms were proposed to account for the ion acceleration in a vacuum spark discharge: acceleration by electrons in an expanding plasma [98, 127], acceleration of a plasma bunch with a frozen-in magnetic flux [128], etc. Most of them coincide with the mechanisms suggested to interpret the collective ion acceleration in the REB propagation through a neutral gas (see Section 3). Regrettably, the above-listed models consider the accelerating process in isolation from the observed physical effects in the aggregate, and therefore these suggestions are quite often in disagreement with the available experimental data.

Barengol'ts et al. [129] made an attempt to unify the basic processes accompanying the development of a spark discharge in vacuum in order to obtain an integral picture of the phenomenon under investigation. They came up with an electrostatic model wherein ions in a vacuum discharge are accelerated in the deep nonstationary VC potential well. This model was used successfully to account for the collective ion acceleration in the electron beam injection into a neutral gas [81] and, in Olson's opinion, could be applied to diodes as well. Barengol'ts et al. [129] showed the possibility of producing a deep potential well in the current injection into a diode gap not only for a zero applied potential, but also in the presence of an electric field in the gap. The proposed model of current flow and potential-well production in a vacuum diode was constructed with the inclusion of an ectonic mechanism of cathode spot operation, i.e. the portion-wise nature of explosive electron emission from the cathode, and is in good agreement with the experimental evidences.

5.2 Collective ion acceleration mode with traveling boundary of a distributed VC

Among the collective acceleration schemes considered above, the systems with a traveling VC hold the greatest promise for high-energy ion beam production. Grouped with these systems are gas-filled vircators [56] and vacuum vircators with ion extraction from the anode (the Luce diode or the vircator with a plasma anode) [96, 103]. In systems with a traveling VC, the energy gained by ions is in direct relation to the time period wherein there persists the synchronism between the VC and the ions embedded in it. In the above two vircator schemes, the directed VC motion is due to the gradual neutralization of the negative space charge of the VC by the ions entering it. In other words, were it not for the ions, the VC would remain immobile on the average. Consequently, the ion acceleration rate is hardly possible to control in these vircators. In this connection, several promising acceleration schemes were developed, in which the VC can move independently and its velocity is controllable.

One of such schemes was proposed by Lymar' et al. [130 – 132] who considered the technique of collective ion acceleration by the field of a traveling distributed-VC boundary. A schematic diagram of the accelerating device for the realization of this technique is given in Fig. 17. Here, the electron beam with a supercritical current is injected into the drift space to produce the VC simultaneously through the whole length of the acceleration region. Then, in the accelerating

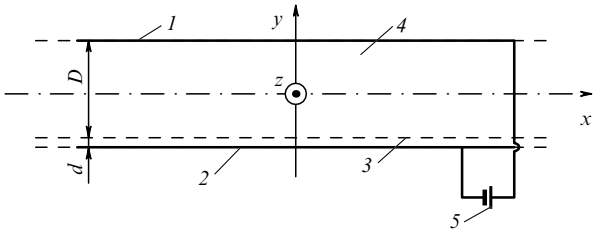

Figure 17. Schematics of the accelerating device: (*1*) collector, (*2*) cathode, (*3*) mesh anode, (*4*) electron drift space (accelerating channel), (*5*) power supply [132].

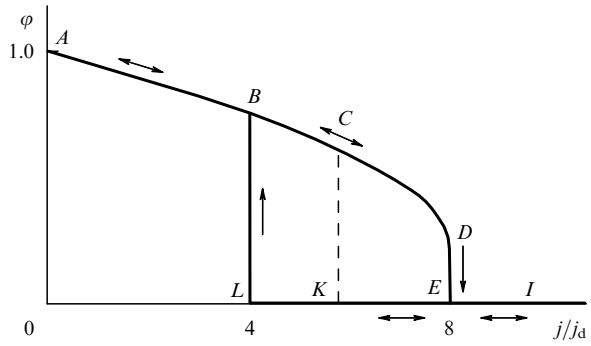

Figure 18. Reduced minimal value of the potential in the drift space as a function of the reduced injection current density [132].

channel there forms a wave of electron beam transition from the state with a VC to a state with a current of purely transit electrons, this wave propagating in the x-direction. Ions are accelerated by the field of precisely this wave. The state of the electron beam in the accelerating channel is determined by the density of a current injected into it. For a given potential difference U_0 between the cathode and the anode and a given A – C gap width d, this density can be varied in the limits between zero and $j_{e\,\max} = 4\varepsilon_0(2e/m)^{1/2}U_0^{3/2}/9d^2$ by varying the temperature and accordingly the emissive capacity of the cathode. In some range of j_e, there occurs a hysteresis of the electron beam states (Fig. 18), whose properties are used to generate the switching wave.

Latsko [133] came up with a practically similar idea which lies in the fact that a chain of several VCs is produced along the ion acceleration axis with the aid of the sequence of electronic diodes. Then, as the ion beam travels along the acceleration axis, an external device switches each electronic gap from the state with a VC to the state without it. In this case, the rear front of this chain can be made to move in synchronism with the ion beam being accelerated.

In principle, the synchronism of collective ion acceleration and the modular accelerator design afford the acceleration of ions to arbitrarily high energies. However, the realization of these methods is related to a specific technical feature which complicates these projects. The matter is that the accelerated ion beam and the VC-producing electron beams move, according to Refs [130 – 133], in mutually perpendicular directions. Magnetic systems of beam tracking are hence inapplicable in this case. This in turn casts doubt on the possibility of constructing the long accelerating channels on the basis of these schemes. Furthermore, among the disadvantages of the approach made in Ref. [133] is the extreme complexity of its practical implementation. An accelerator realizing this approach should ensure, first, programmable high-current, high-voltage switching with a subnanosecond precision and, second, the production of a rather complex configuration of quasi-stationary magnetic and electric fields in the region of electron acceleration and focusing, as well as along the axis of ion acceleration.

The authors of the present review proposed several techniques of collective ion acceleration free from the above disadvantages. These techniques involve ion beam injection along the accelerating channel, thereby making possible the magnetic tracking of the electron and ion beams.

The first technique [134] is based on the effect of hysteresis of the electron flow states in the drift space and the effect of charge dumping in going over from one state to another [135]. As shown in Refs [135, 136], several states of the electron beam are possible, depending on the value of the parameter $q = 4\pi e^2 n_0 d^2/mV_0^2$ (n_0 and V_0 are the electron number density and velocity in the injection into the equipotential gap, and d is the gap width) (Fig. 19).

As the q parameter increases from 0 to 16/9, the electron beam successively passes through the states corresponding to the points A, B, and C. On further increase in q, at point C there occurs a break of the stationary state and the electron flow goes over to a transient (oscillatory) state with a VC (conventionally shown with a wavy line in Fig. 19). The upper CD branch of the curve corresponds to the unstable state which is not realized. In the reverse reduction of $q < 16/9$, the electron flow remains nonstationary with the VC. When q is lowered to 8/9, the electron flow comes to the state corresponding to point D. On further reduction of q, the electron flow experiences a jumpwise transition from the D state to the B state. This jump is accompanied with electric charge dumping and is the crucial point in the proposed ion acceleration technique [134], whose physical essence consists in a synchronous charging of the electron current jump with ions. In the practical implementation of the technique, the instant of positive ion injection is related to the instant of disappearance of the microwave radiation.

In the methods adopted in Refs [130 – 133], the effect of charge dumping and the corresponding jump of the electron current should also be exhibited in the transition of the electron flow from the state with a VC to the state without the VC. However, this effect is hard to harness, because in this case the charge dumping takes place in the direction perpendicular to the ion acceleration axis.

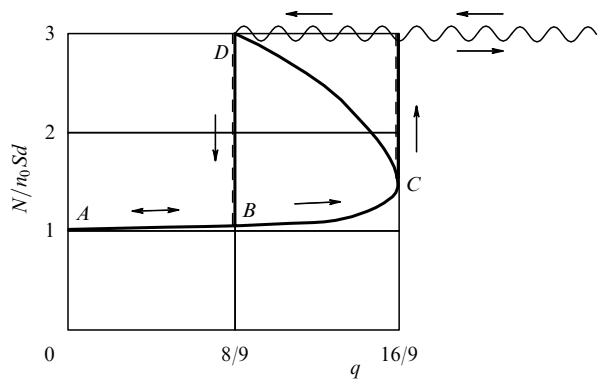

Figure 19. Total number of electrons in the equipotential gap as a function of the parameter q [134].

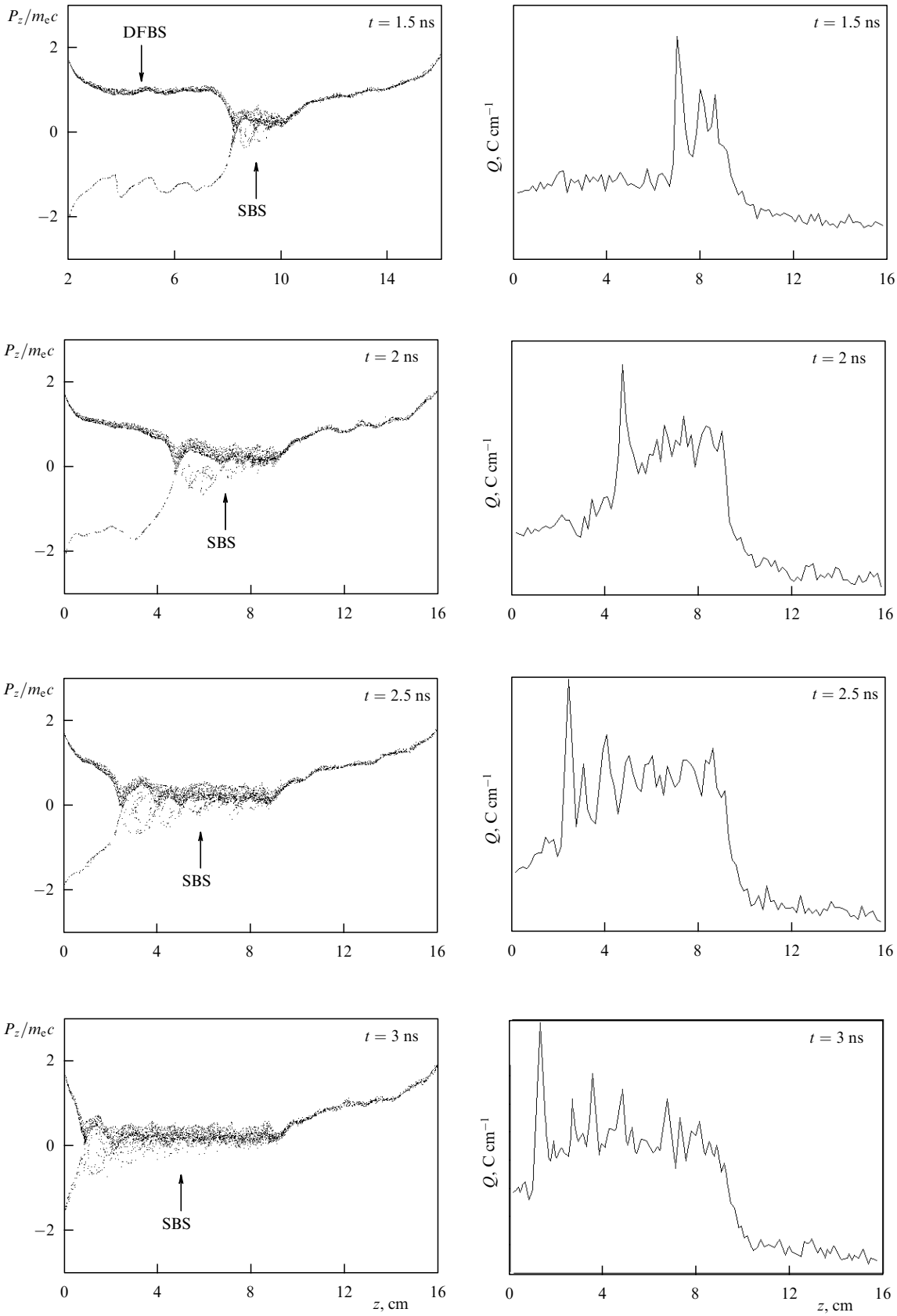

Figure 20. Wave-like character of SBS settling: time evolution of the beam phase portrait (left), and time evolution of the charge distribution along the beam axis (right).

The second promising approach proposed by the authors of the present review considers collective ion acceleration in the mode of the traveling boundary of a distributed VC. It is based on the effect of transition from the double-flow beam

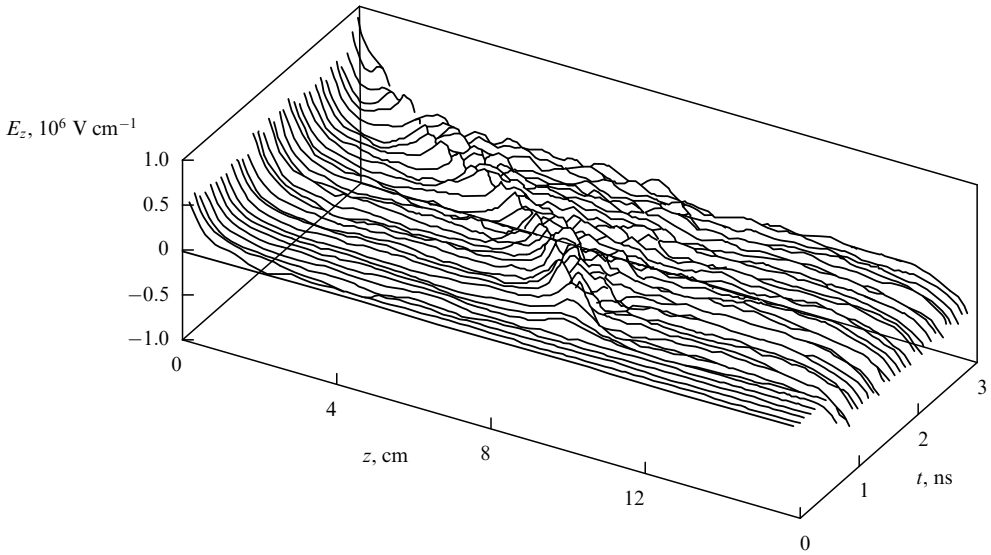

Figure 21. Spatiotemporal dynamics of the longitudinal electric field.

state (DFBS) to the so-called 'squeezed beam state' (SBS), which was discovered in Ref. [137] and is characterized by a low electron velocity and a high electron number density, as well as a developed turbulence of the counterrunning flows. This transition occurs in electron beams with $I > I_{\text{lim}}$. As found in Ref. [134], in a foil-free magnetically insulated vircator, which is a long tube with a jump in diameter, the SBS formation is wave-like in character. In this case, the DFBS $\rightarrow$ SBS switching wave travels in the direction from the VC to the cathode, i.e. in opposition to the direction of electron beam injection. The switching wave velocity was estimated at about 10^{10} cm s^{-1}. A theory was proposed to account for this effect, which is based on the balance of the moments of pressure forces in the sections on opposite sides of the diameter jump, i.e. the SBS is actually a VC distributed over the drift region space.

The investigation of SBS settling dynamics was continued in works [138–140]. The calculated results of Ref. [138] showed that the switching wave velocity lowers when a foil or a thin plasma layer is placed at the diameter jump in a magnetically insulated vircator. It was discovered in Ref. [139] that the switching wave in a magnetically insulated vircator with a magnetic mirror can travel away from the cathode.

The propagation dynamics of an SBS settling wave was calculated for a magnetically insulated vircator with the following parameters: $I = 10$ kA, $U_0 = 750$ kV, $B = 50$ kG. The calculated data were represented in the form of several phase portraits of the beam and instantaneous profiles of electron space charge, synchronized with the former (Fig. 20). An analysis of the profiles shows that there is a distinct electron density drop across the switching wave front, and hence a strong longitudinal electric field concentrates here, which is capable of accelerating positive ions. The spatiotemporal pattern of this field, calculated at a radius equal to the external radius of the electron beam, is plotted in Fig. 21.

The calculations suggest that the electric field amplitude at the DFBS $\rightarrow$ SBS switching wave front amounts to several tenths of a megavolt per centimeter. Furthermore, the switching wave velocity is easy to control, for instance, by profiling the channel radius or varying the beam current. Therefore, should the switching wave be charged with an ion bunch, it is possible to ensure its long-duration acceleration at a very high rate. In this case, the magnetic field and the radial potential well produced by the electrons provide the transverse stability of the ions.

This approach shows promise for practical implementations, for it is free from many disadvantages of the above-considered collective ion acceleration techniques and allows realization of the ion accelerators with the stable long-term operating conditions.

6. Conclusions

In our review, we have considered the principal schemes of collective ion acceleration involving electron beams with a VC. The analysis conducted of the operation of these schemes suggests that they hold promise for HPIB production at power levels up to 1 TW.

Diode RSs show promise for high-current HPIB production with voltages of order 1–10 MV and a current $\leqslant 1$ MA, the energy of ions accelerated in them being relatively low (up to several megaelectron-volts). In recent years there arose a demand for producing higher-energy HPIB (up to 1 GeV). Since a VC is, on the average, immobile in diode systems, the total ion acceleration energy will not be high even for a relatively high rate of ion acceleration. Therefore, there is basically no way of obtaining ion beams with substantial energies on the base of diode RSs. This circumstance supposedly accounts for the fact that the last decade hardly saw investigations into these systems.

To generate high-energy ion beams (up to several megaelectron-volts), there is good reason to employ accelerating systems whose operation is based on the effect of a traveling VC. Among them are the gas-filled vircators, vircators with ion production at the anode (the Luce diodes or vircators with a plasma anode), and also novel schemes proposed, which have not gained practical embodiment. These systems have already produced ions with energies up to 45 MeV nucleon^{-1}. However, the further increase in the HPIB energy also encounters some difficulties. The energy gained by ions in the systems with a traveling VC is known to be in direct relation to the period during which the VC moves

in synchronism with the ions. The heart of the problem is therefore to contrive to control the velocity of VC motion.

In the schemes already realized, the cause of directed VC motion lies with the accelerated ions themselves, and controlling the velocity of VC motion in gas-filled vircators and vircators with ion production at the anode is therefore highly conjectural. Several successful attempts [94, 95] were made with gas-filled vircators, which demonstrated the feasibility of controlling the velocity of VC motion. However, they did not receive further development, evidently due to the complexity of controlling the occurring processes. In vircators with ion production at the anode, a method of controlling the velocity of VC motion in longitudinally nonuniform dielectric channels was proposed [118] and technically tested [119]. However, the complexity of calculating the requisite geometry of these channels hampers the practical realization of this approach. This is the credible reason why the investigations of gas-filled vircators and vircators with ion production at the anode were also hardly pursued during the last 10 years.

The advent of new and promising techniques (see Section 5), in which the VC is able to move independently of the ions being accelerated and its velocity of travel is controllable, gives hope that this line of accelerating technology will attract interest anew, due to the possibility of producing higher-energy HPIBs.

This review was written in the context of the RFBR (grant No. 01-02-07016 — analytical review) and ISTC (grant No. 1629) projects.

References

1. Winterberg F *Phys. Rev.* **174** 212 (1968)
2. Vatrunin V E et al., RF Patent No. 2109352 (1998)
3. Ramirez J J, Toepfer A J, Clauser M J *Nucl. Instrum. Methods* **15** 179 (1977)
4. Arteev M S et al. *Kvantovaya Elektron.* **15** 2502 (1988) [*Sov. J. Quantum Electron.* **18** 1570 (1988)]
5. Sarantsev V P, Perel'shteĭn E A *Kollektivnoe Uskorenie Ionov Elektronnymi Kol'tsami* (Collective Ion Acceleration by Electron Rings) (Moscow: Atomizdat, 1979)
6. Humphries S (Jr), Lee J J, Sudan R N *Appl. Phys. Lett.* **25** 20 (1974)
7. Wiley L, Humphries S (Jr), Sudan R N *Bull. Am. Phys. Soc.* **21** 691 (1976)
8. Humphries S (Jr), Sudan R N, Wiley L *J. Appl. Phys.* **47** 2382 (1976)
9. Agafonov A V, Krastelev E G *At. Tekh. za Rubezhom* **23** (4) 9 (1979)
10. Huff R, Smith I *Bull. Am. Phys. Soc.* **35** 848 (1974)
11. Bystritskiĭ V M *Izv. Vyssh. Uchebn. Zaved. Fiz.* **22** (10) 113 (1979)
12. Bystritskiĭ V M, Didenko A N *Usp. Fiz. Nauk* **132** 91 (1980) [*Sov. Phys. Usp.* **23** 576 (1980)]
13. Prono D S et al. *J. Appl. Phys.* **46** 3310 (1975)
14. Creedon J M, Smith I D, Prono D S *Phys. Rev. Lett.* **35** 91 (1975)
15. Antonsen T M (Jr), Ott E *Phys. Fluids* **19** 52 (1976)
16. Ryutov D D, Stupakov G V *Fiz. Plazmy* **2** 566 (1976) [*Sov. J. Plasma Phys.* **2** 309 (1976)]
17. Humphries S (Jr), Sudan R N, Condit W C (Jr) *Appl. Phys. Lett.* **26** 667 (1975)
18. Humphries S (Jr), Lee J J, Sudan R N *J. Appl. Phys.* **46** 187 (1975)
19. Prono D S, Shearer J W, Briggs R J *Phys. Rev. Lett.* **37** 21 (1976)
20. Kapetanakos C A, Golden J, Black W M *Phys. Rev. Lett.* **37** 1236 (1976)
21. Golden J, Kapetanakos C A *Appl. Phys. Lett.* **28** 3 (1976)
22. Okada C et al. *Jpn. J. Appl. Phys.* **15** 1615 (1976)
23. Bystritskiĭ V M et al., in *Trudy V Vsesoyuz. Soveshch. po Uskoritelyam Zaryazhennykh Chastits, Dubna, 5–7 Oktyabrya 1976 g.* (Proc. of the Vth All-Union Workshop on Charged Particle Accelerators, Dubna, 5–7 October 1976) Vol. 1 (Moscow: Nauka, 1977) p. 391
24. Young F C, Golden J, Kapetanakos C A *Rev. Sci. Instrum.* **48** 432 (1977)
25. Bystritskiĭ V M, Krasik Ya E, Podkatov V I *Zh. Tekh. Fiz.* **49** 2417 (1979) [*Sov. Phys. Tech. Phys.* **24** 1352 (1979)]
26. Bystritskiĭ V M, Krasik Ya E *Fiz. Plazmy* **6** 413 (1980) [*Sov. J. Plasma Phys.* **6** 227 (1980)]
27. Didenko A N et al. *Pis'ma Zh. Tekh. Fiz.* **5** 321 (1979) [*Sov. Tech. Phys. Lett.* **5** 128 (1979)]
28. Pasour J A et al. *Phys. Rev. Lett.* **40** 448 (1978)
29. Mahaffey R A et al. *Appl. Phys. Lett.* **32** 522 (1978)
30. Arbuzov A I, Bystritskiĭ V M, Nauk M D *Zh. Tekh. Fiz.* **53** 402 (1983)
31. Arbuzov A I, Bystritskiĭ V M, Krasik Ya E *Izv. Vyssh. Uchebn. Zaved. Fiz.* **23** (5) 113 (1981)
32. Arbuzov A I, Bystritskiĭ V M *Zh. Tekh. Fiz.* **51** 2383 (1981)
33. Didenko A N et al. *Zh. Tekh. Fiz.* **54** 816 (1984) [*Sov. Phys. Tech. Phys.* **29** 482 (1984)]
34. Bystritskiĭ V M et al. *Fiz. Plazmy* **12** 1113 (1986)
35. Borisenok V A et al., in *Rossiĭskiĭ Seminar "Sovremennye Sredstva Diagnostiki Plazmy i Ikh Primenenie dlya Kontrolya Veshchestv i Okruzhayushcheĭ Sredy", Moskva, 8–9 Iyunya 1998 g.* (Proc. of the Russian Seminar "Modern Techniques of Plasma Diagnostics and their Application to Environmental and Materials Monitoring", Moscow, 8–9 June, 1998) (Moscow: Izd. MIFI, 1998) p. 20
36. Donets E D *Fiz. Elem. Chastits At. Yadra* **13** 941 (1982)
37. Bystritskiĭ V M et al. *Zh. Tekh. Fiz.* **55** 2040 (1985)
38. Bystritskiĭ V M, Volkov S N, Krasik Ya E *Fiz. Plazmy* **12** 1314 (1986)
39. VanDevender J P, Stinnett R W, Anderson R J *Appl. Phys. Lett.* **38** 229 (1981)
40. Agafonov A V et al. *Zh. Eksp. Teor. Fiz.* **84** 2040 (1983) [*Sov. Phys. JETP* **57** 1188 (1983)]
41. Andrews M L et al. *Phys. Rev. Lett.* **27** 1428 (1971)
42. Bzura J J et al. *Phys. Rev. Lett.* **29** 256 (1972)
43. Sudan R N, Ott E *Phys. Rev. Lett.* **33** 355 (1974)
44. Kapetanakos C A, Golden J, Young F C *Nucl. Fusion* **16** 151 (1976)
45. Golden J et al. *Phys. Rev. Lett.* **38** 130 (1977)
46. Clauser M J *Phys. Rev. Lett.* **35** 848 (1975)
47. Kawata S et al. *J. Phys. Soc. Jpn.* **47** 1651 (1979)
48. Bystritskiĭ V M, Ivanov I B, Petrov A V *Zh. Tekh. Fiz.* **56** 801 (1986)
49. Mahaffey R A et al. *Phys. Rev. Lett.* **39** 843 (1977)
50. Hoeberling R F, Fazio M V *IEEE Trans. Electromagn. Comp.* **34** 252 (1992)
51. Didenko A N et al. *Pis'ma Zh. Tekh. Fiz.* **9** 1510 (1983) [*Sov. Tech. Phys. Lett.* **9** 647 (1983)]
52. Grigor'ev V P et al. *Fiz. Plazmy* **14** 210 (1988)
53. Rukhadze A A, Stolbetsov S D, Tarakanov V P *Radiotekh. Elektron.* **37** 385 (1992)
54. Yuferov V et al., in *12th IEEE Intern. Pulsed Power Conf., Monterey, CA, USA, June 27–30, 1999*, Digest of technical papers Vol. 2 (Monterey, CA: IEEE, 1999) p. 845
55. Yuferov V B et al. *Vopr. At. Nauki Tekh. Ser. Plazm. Elektron. Novye Metody Uskor.* (1) 146 (2000)
56. Uglum J R, Graybill S *J. Appl. Phys.* **41** 236 (1970)
57. Rander J et al. *Phys. Rev. Lett.* **24** 283 (1970)
58. Graybill S E *IEEE Trans. Nucl. Sci.* **NS-18** 438 (1971)
59. Yonas G *IEEE Trans. Nucl. Sci.* **NS-19** 297 (1972)
60. Ecker B, Putnam S, Drickey D J *IEEE Trans. Nucl. Sci.* **NS-20** 301 (1973)
61. Kuswa G W, Bradley L P, Yonas G *IEEE Trans. Nucl. Sci.* **NS-20** 305 (1973)
62. Straw D C, Miller R B *Appl. Phys. Lett.* **25** 379 (1974)
63. Straw D C, Miller R B *J. Appl. Phys.* **47** 4681 (1976)
64. Kolomenskiĭ A A et al. *Zh. Eksp. Teor. Fiz.* **68** 51 (1975) [*Sov. Phys. JETP* **41** 23 (1975)]
65. Bystritskiĭ V M et al. *Pis'ma Zh. Tekh. Fiz.* **2** 80 (1976) [*Sov. Tech. Phys. Lett.* **2** 30 (1976)]
66. Bystritskiĭ V M, Podkatov V I *Zh. Tekh. Fiz.* **52** 1608 (1982)
67. Agafonov A V *At. Tekh. za Rubezhom* **18** (4) 32 (1974)
68. Gapanovich V G, Kolomenskiĭ A A *Izv. Vyssh. Uchebn. Zaved. Fiz.* **22** (10) 59 (1979)
69. Bogdankevich L S, Rukhadze A A *Usp. Fiz. Nauk* **103** 609 (1971) [*Sov. Phys. Usp.* **14** 163 (1972)]

70. Rostoker N *Bull. Am. Phys. Soc.* **14** 1047 (1969)
71. Rostoker N, in *Trudy VII Mezhd. Konf. po Uskoritelyam Zaryazhennykh Chastits Vysokoĭ Energii, Erevan, 27 Avgusta – 2 Sentyabrya 1970 g.* (Proc. VIIth Int. Conf. High-En. Charged-Part. Accelerators, Erevan, 27 Aug. – 2 Sept. 1970) Vol. 2 (Erevan: Izd. AN Arm. SSR, 1970) p. 509
72. Wachtel J M, Eastlund B J *Bull. Am. Phys. Soc.* **14** 1047 (1969)
73. Putnam S D *Bull. Am. Phys. Soc.* **14** 1048 (1969)
74. Putnam S D *Phys. Rev. Lett.* **25** 1129 (1970)
75. Uglum J R, Graybill S E, McNeill W H *Bull. Am. Phys. Soc.* **14** 1047 (1969)
76. Khodataev K V, Tsytovich V N *Fiz. Plazmy* **2** 301 (1976) [*Sov. J. Plasma Phys.* **2** 164 (1976)]
77. Rosinskiĭ S E, Rukhadze A A, Rukhlin V G *Pis'ma Zh. Tekh. Fiz.* **14** 53 (1971)
78. Alexander K, Hantzsche E, Siemroth P *Zh. Eksp. Teor. Fiz.* **67** 567 (1974) [*Sov. Phys. JETP* **40** 283 (1975)]
79. Kucherov V I *Pis'ma Zh. Tekh. Fiz.* **1** 235 (1975)
80. Poukey J W, Olson C L *Phys. Rev. A* **11** 691 (1975)
81. Olson C L *Phys. Rev. A* **11** 288 (1975)
82. Gapanovich V G, Kolomenskiĭ A A, Logachev I I, in *Tezisy Dokladov III Vsesoyuznogo Simpoziuma po Sil'notochnoĭ Impul'snoĭ Elektronike* (Proc. of the IIIrd All-Union Symposium on High-Current Pulsed Electronics) (Tomsk: Institut Sil'notochnoĭ Elektroniki, 1978) p. 190
83. Straw D C, Miller R B, Hoeberling R F *Bull. Am. Phys. Soc.* **21** 1101 (1976)
84. Mako R W, Fisher A *Bull. Am. Phys. Soc.* **21** 1059 (1976)
85. Roberson C W et al. *Phys. Rev. Lett.* **36** 1457 (1976)
86. Kolomenskiĭ A A, Novitskiĭ M A *Zh. Tekh. Fiz.* **46** 44 (1976)
87. Khodataev K V, Shakhanova E V *Fiz. Plazmy* **13** 1035 (1987)
88. Ginzburg S L et al., Preprint No. 37 (Moscow: M.V. Keldysh Institute for Applied Mathematics, USSR Academy of Sciences, 1981)
89. Ginzburg S L, D'yachenko E F, Khodataev K V, Preprint No. 65 (Moscow: M.V. Keldysh Institute for Applied Mathematics, USSR Academy of Sciences, 1982)
90. Shakhanova E V, Preprint No. 106 (Moscow: M.V. Keldysh Institute for Applied Mathematics, USSR Academy of Sciences, 1983)
91. Ginzburg S L et al., Preprint No. 72 (Moscow: M.V. Keldysh Institute for Applied Mathematics, USSR Academy of Sciences, 1983)
92. Tkach Yu V et al. *Zh. Tekh. Fiz.* **44** 658 (1974)
93. Khodataev K V, Ginzburg S L, D'yachenko E F, Preprint No. 138 (Moscow: M.V. Keldysh Institute for Applied Mathematics, USSR Academy of Sciences, 1984)
94. Olson C L et al. *IEEE Trans. Nucl. Sci.* **NS-30** 3189 (1983)
95. Olson C L et al. *Phys. Rev. Lett.* **56** 2260 (1986)
96. Luce J S, Sahlin H L, Crites T R *IEEE Trans. Nucl. Sci.* **NS-20** 336 (1973)
97. Korop E D, Plyutto A A *Zh. Tekh. Fiz.* **40** 2534 (1970)
98. Plyutto A A *Zh. Tekh. Fiz.* **39** 1589 (1960)
99. Plyutto A A et al. *Pis'ma Zh. Eksp. Teor. Fiz.* **6** 540 (1967) [*JETP Lett.* **6** 80 (1967)]
100. Zorn G T, Kim H, Boyer C N *IEEE Trans. Nucl. Sci.* **NS-22** 1006 (1975)
101. Bystritskiĭ V M et al. *Pis'ma Zh. Tekh. Fiz.* **4** 547 (1978)
102. Vijayan T, Roychowdhury P, Iyyengar S K *IEEE Trans. Plasma Sci.* **PS-22** 199 (1994)
103. Babkin A L et al., in *Issledovaniya po Fizike Plazmy* (Plasma Physics Research) (Trudy Uchebnykh Yadernykh Tsentrov Rossii (Proceedings of Scientists from Russian Nuclear Centers), Vol. 6, Eds V D Selemir, A E Dubinov) (Sarov: RFYaTs – VNIIEF, 1998) p. 173
104. Chelpanov V I et al., in *12th IEEE Intern. Pulsed Power Conf., Monterey, CA, USA, June 27 – 30, 1999*, Digest of technical papers Vol. 2 (Monterey, CA: IEEE, 1999) p. 1025
105. Vijayan T, Roychowdhury P *IEEE Trans. Plasma Sci.* **PS-28** 2166 (2000)
106. Boyer C N, Kim H, Destler W W *IEEE Trans. Nucl. Sci.* **NS-24** 1625 (1977)
107. Destler W W, Floyd L E, Reiser M *Phys. Rev. Lett.* **44** 70 (1980)
108. Faĭnberg Ya B, in *Kollektivnye Metody Uskoreniya: Materialy Konf. po Yaderno-Fizicheskim Issledovaniyam, Posvyashchennoĭ 50-letiyu Osushchestvleniya v SSSR Reaktsii Rasshchepleniya Atomnogo Yadra, Khar'kov, 4 – 6 Oktyabrya 1982* (Collective Acceleration Techniques: Proceedings of the Nuclear Physics Research Conference Dedicated to the 50th Anniversary of Realization of Atomic Nuclear Fission Reaction in the USSR, Khar'kov, 4 – 6 October 1982) Pt. I (Moscow: TsNIIatominform, 1983) p. 222
109. Dolgopolov V V et al. *Ukr. Fiz. Zh.* **34** 1164 (1989)
110. Stepanenko I A, Tkach Yu V, Pashchenko A V, Preprint No. 88-37 (Khar'kov: Khar'kov Institute of Physics and Technology, Academy of Sciences of the Ukrainian SSR, 1988)
111. Dolgopolov V V et al. *Ukr. Fiz. Zh.* **42** 536 (1997)
112. Adler R J, Nation J A *J. Appl. Phys.* **50** 5025 (1979)
113. Adler R, Nation J A, Serlin V *Phys. Fluids* **24** 347 (1981)
114. Godfrey B B, Thode L E *IEEE Trans. Plasma Sci.* **PS-3** 201 (1975)
115. Davidson R C et al. *Phys. Rev. Lett.* **24** 579 (1970)
116. Hoeberling R F, Payton III D N *J. Appl. Phys.* **48** 2079 (1977)
117. Johnson D J, Kerns J R *Appl. Phys. Lett.* **25** 192 (1974)
118. Choe J Y, Uhm H S *IEEE Trans. Nucl. Sci.* **NS-30** 3174 (1983)
119. Aĭrapetov A Sh et al., in *Soveshchanie po Problemam Kollektivnogo Metoda Uskoreniya, Dubna, 18 – 20 Maya 1982* (Workshop on the Problems of Collective Acceleration Technique, Dubna, 18 – 20 May 1982) (Dubna: Izd. OIYaI, 1982) p. 111
120. Dubinov A E, Kornilova I Yu *Izv. Vyssh. Uchebn. Zaved. Fiz.* **44** (6) 71 (2001) [*Russ. Phys. J.* **44** 646 (2001)]
121. Tarakanov V P *User's Manual for Code KARAT* (Springfield, VA: Berkeley Research Associates, Inc., 1992)
122. Anfinogentov V G, Khramov A E *Izv. Ross. Akad. Nauk Ser. Fiz.* **62** 2428 (1998)
123. Kurilko V I, Faĭnberg Ya B *Pis'ma Zh. Tekh. Fiz.* **2** 397 (1976)
124. Balakirev V A et al. *Fiz. Plazmy* **23** 350 (1997) [*Plasma Phys. Rep.* **23** 323 (1997)]
125. Plyutto A A et al. *At. Energ.* **27** 418 (1969)
126. Plyutto A A et al. *Zh. Tekh. Fiz.* **43** 1627 (1973)
127. Gurevich A V, Pariĭskaya L V, Pitaevskiĭ L P *Zh. Eksp. Teor. Fiz.* **63** 516 (1972) [*Sov. Phys. JETP* **36** 274 (1973)]
128. Korop E D *Zh. Tekh. Fiz.* **46** 2187 (1976)
129. Barengol'ts S A, Mesyats G A, Perel'shtein É A *Zh. Eksp. Teor. Fiz.* **118** 1358 (2000) [*JETP* **91** 1176 (2000)]
130. Lymar' A G et al., USSR Author's Certificate No. 1263187 (1976)
131. Lymar' A G, Zvyagintsev A V, Khizhnyak N A, Preprint No. 88-1 (Khar'kov: Khar'kov Institute of Physics and Technology, Academy of Sciences of the Ukrainian SSR, 1988)
132. Lymar' A G et al. *Vopr. At. Nauki Tekh. Ser. Yaderno-Fiz. Issled.* (5) 71 (1989)
133. Latsko E M, USSR Author's Certificate No. 1529476 (1989)
134. Dubinov A E, RF Patent No. 2171017 (2001)
135. Pashchenko A V, Rutkevich B N *Zh. Tekh. Fiz.* **53** 75 (1983)
136. Dubinov A E *Vopr. At. Nauki Tekh. Ser. Teor. Prikl. Fiz.* (2) 3 (2001)
137. Ignatov A M, Tarakanov V P *Phys. Plasmas* **1** 741 (1994)
138. Dubinov A E *Pis'ma Zh. Tekh. Fiz.* **23** (22) 29 (1997) [*Tech. Phys. Lett.* **23** 870 (1997)]
139. Dubinov A E *Radiotekh. Elektron.* **45** 875 (2000) [*J. Commun. Technol. El.* **45** 792 (2000)]
140. Dubinov A E, Efimova I A *Zh. Tekh. Fiz.* **71** (6) 80 (2001) [*Tech. Phys.* **46** 723 (2001)]